Novel Mechanism of Fasting Response in Pancreatic ß Cells

Author(s):
Goginashvili, Alexander

Publication Date:
2014

Permanent Link:

https://doi.org/10.3929/ethz-a-010209056 →

DISS. ETH NO. 21906

NOVEL MECHANISM

OF FASTING RESPONSE IN PANCREATIC β CELLS

A thesis submitted to attain the degree of

DOCTOR OF SCIENCES of ETH ZURICH

(Dr. sc. ETH Zurich)

presented by

Alexander Goginashvili

Master of Science in Biology, Saint-Petersburg State University, Russian Federation

born on November 30th, 1984

citizen of the Russian Federation

accepted on the recommendation of

Prof. Dr. Ernst Hafen,

Prof. Dr. Romeo Ricci,

Prof. Dr. Robbie Loewith

2014

1. Table of Contents

2. Detailed Table of Contents

3. List of figures

4. Abbreviations

4E-BP	Eukaryotic translation initiation factor 4E-binding protein
AMBRA1	Activating molecule in BECN1-regulated autophagy protein 1
AMPK	5' Adenosine monophosphate-activated protein kinase
ATG	Autophagy-related gene
BAR	Bin–Amphiphysin–Rvs
CAD	Carbamoyl-phosphate synthetase 2, Aspartate transcarbamoylase, and Dihydroorotase
CLEM	Correlative light and electron microscopy
DAP1	Death-associated protein 1
FIP200	FAK family kinase-interacting protein of 200 kDa
FLCN	Folliculin
FRET	Fluorescence resonance energy transfer
GABA	γ-aminobutyric acid
GABARAP	γ-aminobutyric acid (GABA) receptor-associated protein (GABARAP)
GABARAPL2	γ -aminobutyric acid (GABA) receptor-associated protein-like 2
GAP	guanosine triphosphatase (GTPase)-activating protein
GATE16	Golgi-associated ATPase enhancer of 16 kDa

GATOR	GTPase-activating protein (GAP) activity toward Rags
GEF	Guanine nucleotide exchange factors
GTPase	Guanosine Triphosphatase
LeuRS	Leucyl-tRNA synthetase
MAP1LC3	Microtubule-associated protein 1 light chain 3
MAP4K3	Mitogen-activated protein kinase kinase kinase kinase 3
mTOR	mammalian (or mechanistic) Target Of Rapamycin
mTORC1	mTOR Complex I
PAT1	Proton-coupled amino acid transporter 1
PE	Phosphatidylethanolamine
Phogrin	Phosphatase homologue of granules from rat insulinoma
PI(3)K	Phosphatidylinositol-3-OH kinase
PKD1	Protein Kinase D1
PM	Plasma membrane
PPP	Pentose Phosphate Pathway
PtdIns(3)P	Phosphatidylinositol-3-phosphate
QEM	Quantitative electron microscopy
Rag	Ras-related GTP-binding protein

RB1CC1	RB1-inducible coiled-coil protein 1
RER	Rough endoplasmic reticulum
Rheb	Ras homolog enriched in brain
S6K	Ribosomal protein S6 kinase
SG	Secretory Granule
SINGD	Starvation-Induced Nascent Granule Degradation
SNAP-29	Synaptosomal-associated protein 29
SNARE	Soluble NSF Attachment Protein (SNAP) Receptor
SREBP	Sterol Regulatory Element Binding Protein
TEM	Transmission electron microscopy
TGN	Trans-Golgi Network
TRAF6	TNF receptor-associated factor 6
TSC	tuberous sclerosis
TTT-RUVBL1/2	Tel2-Tti1-Tti2-RuvB-like protein 1/2
Ubl	Ubiquitin-like
ULK	Unc-51-like kinase
VAMP8	Vesicle-associated membrane protein 8
v-ATPase	vacuolar H^+–adenosinetriphosphatase

VPS15	Vacuolar protein sorting-associated protein 15
VPS34	Vacuolar protein sorting-associated protein 34
WIPI2	WD repeat domain phosphoinositide-interacting protein 2
4E-BP	Eukaryotic translation initiation factor 4E-binding protein

5. Zusammenfassung

Die Verfügbarkeit von Nährstoffen ist grundlegend für das Gleichgewicht zwischen Anabolismus und Katabolismus in Säugetierzellen. Im momentanen Verständniß der Zellbiologie führt ein Mangel von extrazellulären Nährstoffen zur Makroautophagie. Dies ist ein vorrangig katabolischer Prozess, bei dem Nährstoffe aus dem Abbau zellulärer Bestandteile gewonnen werden, um so das Überleben der Zelle zu sichern. In der hier vorliegenden Arbeit habe ich herausgefunden, dass β-Zellen des Pankreas, welche eine Schlüsselfunktion im Stoffwechsel von Säugetieren übernehmen, einen anderen und bisher unbekannten Mechanismus aufzeigen, um sich einem Mangel an Nährstoffen anzupassen. Bei einem Entzug von Nährstoffen, werden in β-Zellen reifende Insulin-haltige Granula abgebaut, indem sie mit Lysosomen in der Nähe des Golgi-Apparates fusionieren. Diesen Prozess werde ich im Verlauf als „Starvation-Induced Nascent Granule Degradation“ (SINGD) bezeichnen. Der zelluläre Sensor für Nährstoffe, mTORC1, bindet dann die Lysosomen, wodurch er lokal aktiviert wird und somit die Makroautophagie inhibiert. Zudem zeige ich, dass SINGD von der Protein Kinase D1 (PKD1), einem wichtiger Regulator der Insulin-Granula Bildung am Trans-Golgi-Netzwerk, reguliert wird. Die Aktvierung von SINGD bei Nährstoffmangel wird durch eine schnelle Inaktivierung von PKD1 am Trans-Golgi Netzwerk ausgelöst. Das zeigt, dass sich ß-Zellen im Gegensatz zu den meisten anderen Zelltypen nicht mit Hilfe der Makroautophagie an Nährstoffmangel anpassen, sondern die Funktion des Golgi modifizieren.

Viele Stoffwechselprodukte die bei einer Makroautophagie gebildet werden, verstärken die Freisetzung von Insulin. Daher würde eine verstärkte Makroautophagie in ß-Zellen die normale Reduktion der Insulin-Freisetzung bei Hunger stören. Tatsächlich führt eine

induzierte Makroautophagie in ß-Zellen auch zu einer erhöhten Insulin Freisetzung trotz Nähstoffmangel. Da ß-Zellen aber vorrangig neugebildete Granula freisetzen, kann SINGD wahrscheinlich das Ausschütten von Insulin begrenzen und verhindert neben der Makroautophagie auch den stimulierenden Effekt durch die neu gebildeten Stoffwechselprodukte. Damit ermöglicht die SINGD-vermittelte Inhibition der Makroautophagie die verminderte Insulin Freisetzung bei Nährstoffmangel.

Zusammengefasst beschreibt der hier entdeckte Mechanismus eine wichtige evolutionäre Anpassung eines spezialisierten sekretorischen Zelltyps der auch in anderen sekretorischen Zellen von Bedeutung sein könnte. Da die Autophagie in ß-Zellen eine wichtige Rolle bei Diabetes spielt, bietet meine Arbeit auch für das Verständnis dieser Krankheit neue und interessante Perspektiven.

6. Summary

Nutrient availability is the major factor determining the balance between anabolic and catabolic reactions in mammalian cells. According to a prevailing concept in cell biology, a shortage of external nutrients results in induction of macroautophagy, a predominant catabolic pathway that supplies metabolites needed for the cell survival through degradation of cellular components. In this study, I have found that pancreatic β cells, key regulators of systemic metabolism in mammals, employ a very distinct and so far unknown mechanism to adapt to nutrient depletion. Starvation of β cells induces selective degradation of nascent insulin secretory granules through their fusion with lysosomes in the Golgi area, a process I will term Starvation-Induced Nascent Granule Degradation (SINGD). The nutrient sensor mTORC1 is recruited to these lysosomes, which leads to its local activation and immediate suppression of macroautophagy upon starvation. Furthermore, I have found that Protein Kinase D1 (PKD1), a major regulator of insulin granule biogenesis at the Trans-Golgi-Network, controls SINGD. Nutrient deprivation leads to a rapid inactivation of PKD1 at the Trans-Golgi-Network, which in turn triggers SINGD. Therefore, macroautophagy is not the strategy of choice in β cells to adapt to nutrient depletion as seen for most other cell types. Instead, the nutrient starvation response is directly linked to Golgi function.

Several metabolites generated through macroautophagy are known to trigger insulin release. Thus, increased macroautophagy in β cells may interfere with fasting-induced suppression of insulin secretion. Indeed, increasing macroautophagy in β cells during starvation enhances insulin secretion. In addition, as β cells preferentially secrete nascent secretory granules, SINGD is likely to limit insulin release, thus compensating stimulatory effects of generated metabolites on the secretion of insulin. Therefore, SINGD-mediated suppression of macroautophagy contributes to fasting-induced suppression of insulin secretion.

Conclusively, the identified mechanism constitutes an important evolutionary adaption in a specialized secretory cell type that could also be important in other secretory cells. Given the important role of autophagy in β cells in the context of diabetes, my study may also offer interesting perspectives in the diabetes field.

7. Introduction

7.1. Mammalian cells sense nutrients to regulate metabolism

The availability of nutrients determines the metabolic activity of cells and organisms. Therefore, proper nutrient sensing is crucial for cell functioning. Mammalian cells sense nutrients on both local (cellular) and systemic (organismal) levels. On the cellular level the cells receive nutrients in the form of glucose, amino acids and other metabolites, while the nutrient status of the organism is translated to the cells through the whole plethora of secreted factors, such as hormones produced by endocrine system. In mammalian cells, several signalling networks collect inputs from nutrients to control catabolic and anabolic pathways (Howell, Ricoult et al. 2013; Yuan, Xiong et al. 2013).

One of the best studied cellular nutrient sensors is the multiprotein mammalian (or mechanistic) Target Of Rapamycin Complex 1 (mTORC1). In presence of nutrients, mTORC1 promotes anabolism through upregulation of protein translation, biosynthesis of lipids and nucleic acids (Wullschleger, Loewith et al. 2006; Laplante and Sabatini 2012; Howell, Ricoult et al. 2013). In particular, mTORC1 promotes lipogenesis through the activation of transcription factor Sterol Regulatory Element Binding Protein (SREBP) via several mechanisms, including inhibition of the phosphatase Lipin1 and activation of the ribosomal S6 Kinase (S6K) (Porstmann, Santos et al. 2008; Duvel, Yecies et al. 2010; Lewis, Griffiths et al. 2011; Peterson, Sengupta et al. 2011; Owen, Zhang et al. 2012).The biosynthesis of nucleic acids (DNA and RNA) is enhanced by mTORC1 through the S6K-dependent phosphorylation of Carbamoyl-phosphate synthetase 2, Aspartate transcarbamoylase, and Dihydroorotase (CAD) and SREBP-dependent transcriptional activation of the Pentose Phosphate Pathway (PPP) (Duvel, Yecies et al. 2010; Ben-Sahra,

Howell et al. 2013; Robitaille, Christen et al. 2013) . mTORC1 upregulates protein synthesis through activation of S6K and inhibition of the eukaryotic translation initiation factor 4E-Binding Protein (4E-BP) that stimulates cap-dependent mRNA translation and biogenesis of ribosomes (Kawasome, Papst et al. 1998; Wang, Li et al. 2001; Laplante and Sabatini 2012; Thoreen, Chantranupong et al. 2012; Chauvin, Koka et al. 2014). The anabolic functions of mTORC1 are summarized in a **Figure I1**.

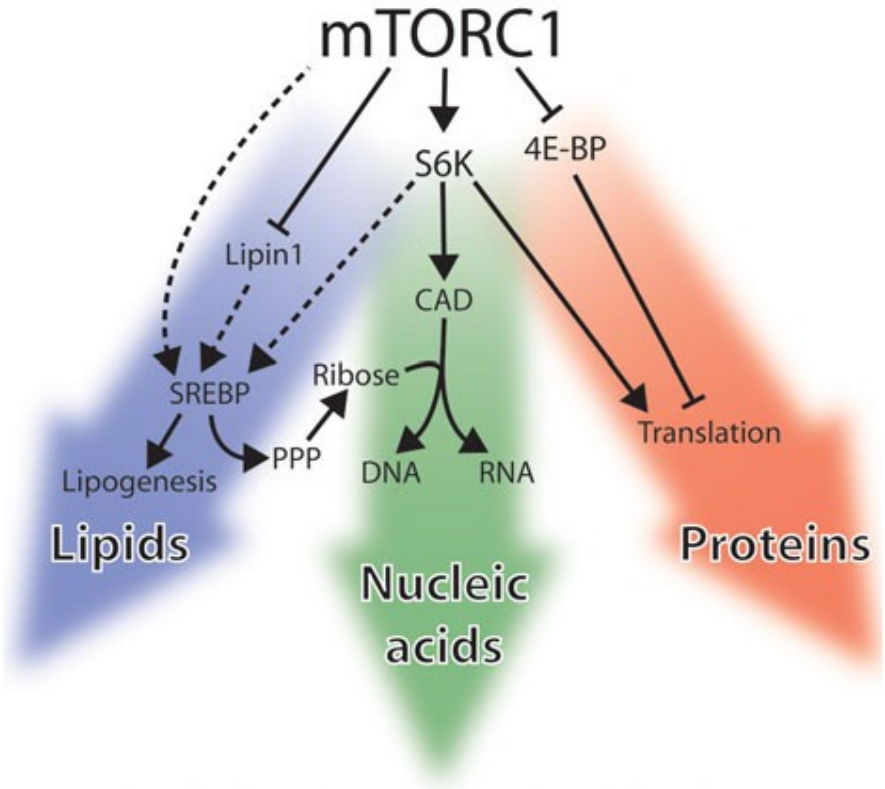

Figure I1. Anabolic functions of mTORC1. Adapted from (Howell, Ricoult et al. 2013)

Alongside with promoting anabolic pathways, mTORC1 inhibits catabolic pathways in the presence of nutrients through suppression of macroautophagy. During macroautophagy (hereafter referred to as "autophagy") cellular proteins and organelles are sequestered into double-membrane autophagosomes that subsequently fuse with lysosomes (autolysosomes),

where degradation occurs. Nutrient deprivation results in decreased mTORC1 activity that in turn leads to induction of autophagy. The catabolites derived from autophagy maintain the cell in a metabolically active state ensuring important cellular functions needed for cell survival (Shintani and Klionsky 2004; Rabinowitz and White 2010; Lamb, Yoshimori et al. 2013). Interestingly, autophagy was shown to re-activate mTORC1 after prolonged nutrient starvation, thus providing a regulatory loop between catabolic and anabolic activities of mTORC1 (see **Figure I2**) (Yu, McPhee et al. 2010).

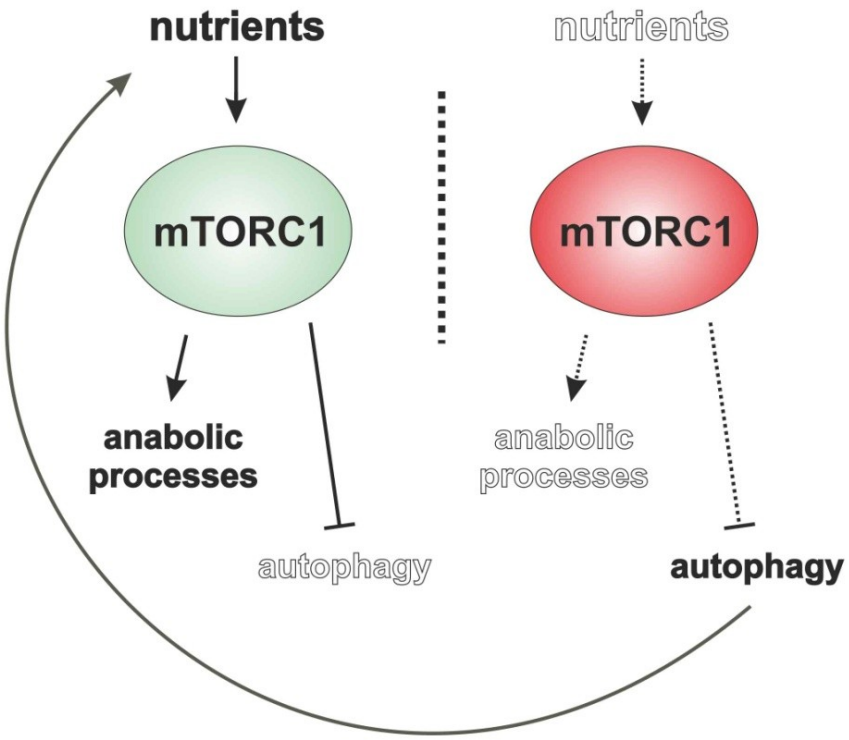

Figure I2. Coordination between anabolic and catabolic branches of mTORC1 pathway

7.2. Control of mTORC1 activity by nutrients

How nutrients, in particular amino acids, regulate mTORC1 activity has remained a conundrum for more than a decade. After publication of first reports on amino acid-sensitive regulation of mTORC1 effectors (Blommaart, Luiken et al. 1995; Hara, Yonezawa et al. 1998), several distinct proteins have been suggested to be important. For instance, type III phosphatidylinositol-3-OH kinase VPS34, Mitogen-activated protein kinase kinase kinase kinase 3 (MAP4K3) and Phospholipase D1 were added to the list of potential regulators of nutrient-dependent activity of mTORC1 (Nobukuni, Joaquin et al. 2005; Findlay, Yan et al. 2007; Xu, Salloum et al. 2011). The model, which dominates now, largely relies on regulation of subcellular localisation of active mTORC1. Based on newly developed antibodies against mTORC1 members, the laboratory of David Sabatini found that amino acids induced translocation of mTORC1 to the membrane of lysosome (Sancak, Peterson et al. 2008; Sancak, Bar-Peled et al. 2010). The laboratories of Sabatini and Kun-Liang Guan revealed that this process is controlled by protein complexes which reside at lysosomal membranes, such as heterodimeric Rag GTPases (Rag A/B bound to Rag C/D) and Ragulator (Kim, Goraksha-Hicks et al. 2008; Sancak, Peterson et al. 2008; Sancak, Bar-Peled et al. 2010) (see **Figure I3**). Amino acids activate Rag GTPases by promoting GTP loading of Rag A/B and GDP loading of Rag C/D. Activated Rags bind Raptor, one of the members of the mTORC1 complex, recruiting mTORC1 to lysosomal membranes. The Ragulator and GATOR1 complexes were identified as a guanine nucleotide exchange factor (GEF) and GTPase-activating protein (GAP) for Rag A/B, respectively (Bar-Peled, Schweitzer et al. 2012; Bar-Peled, Chantranupong et al. 2013), while Folliculin tumor suppressor (FLCN) was shown to serve as a GAP for Rag C/D (Tsun, Bar-Peled et al. 2013). In addition to the amino acid-dependent Rag-mTOR axis, the Rag GTPases were recently found to be involved in

inhibition of mTORC1 by glucose deprivation, thus suggesting that inputs from different nutrients converge into lysosomal activation of mTORC1 (Efeyan, Zoncu et al. 2013).

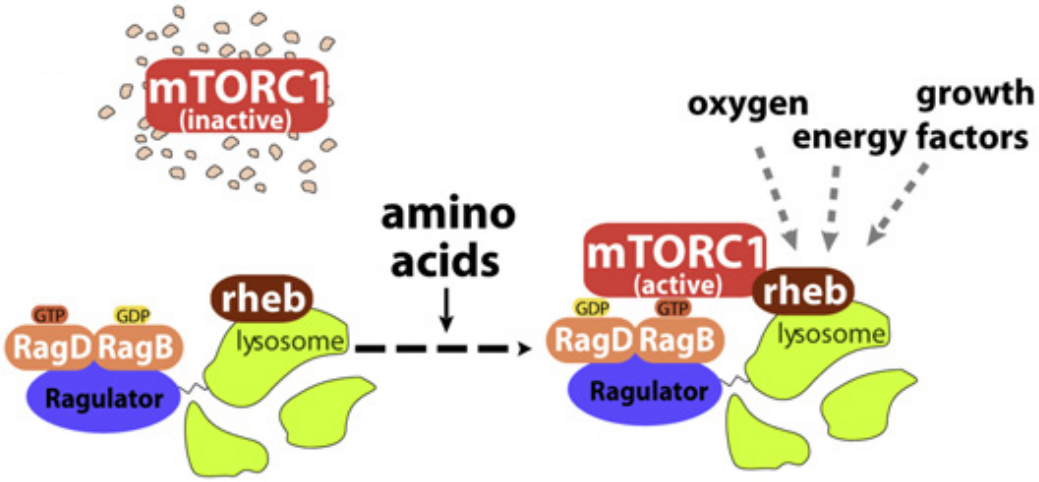

Figure I3. Rags and Ragulator recruit mTORC1 to lysosomes.

Adopted from (Sancak, Bar-Peled et al. 2010)

How is mTORC1 activated on lysosomal membranes? It was shown that lysosomal mTORC1 is activated by another small GTPase, called Rheb, which also resides at lysosomal membrane (Sancak, Peterson et al. 2008; Sancak, Bar-Peled et al. 2010). Rheb is a crucial activator of mTORC1 and it had been extensively studied together with its inhibitor TSC complex (that serves as a GAP for Rheb) as a key player in local and systemic nutrient-dependent mTORC1 regulation (Garami, Zwartkruis et al. 2003; Inoki, Li et al. 2003; Saucedo, Gao et al. 2003; Stocker, Radimerski et al. 2003; Dibble, Elis et al. 2012; Demetriades, Doumpas et al. 2014; Menon, Dibble et al. 2014).

Why does the lysosome serve as a compartment where mTORC1 activation occurs? A possible explanation is that mTORC1 senses nutrients derived from lysosomes. In line with this assumption, the lysosomal amino acid transporter PAT1 was shown to interact with the

Rag GTPases and is required for amino acid-dependent mTOR localisation. Additionally, the Rag-Ragulator complex interacts with the vacuolar H^+–adenosine triphosphatase (v-ATPase), thus linking amino acid sensing to the lysosomal lumen (Zoncu, Bar-Peled et al. 2011; Ogmundsdottir, Heublein et al. 2012). Interestingly, several non-lysosomal amino acid transporters were also shown to be essential for mTORC1 activation (Nicklin, Bergman et al. 2009). It is also possible that certain amino acids specifically control mTORC1 activity upstream of Rags. For instance, leucine was shown to regulate mTORC1 through leucyl-tRNA synthetase (LeuRS) (Han, Jeong et al. 2012); and glutamine, the most abundant amino acid in the blood, was found to induce Rag-dependent mTORC1 activation through its catabolite α-ketoglutarate (Duran, Oppliger et al. 2012).

It is worth pointing out that other mechanisms besides the Rag-Ragulator axis might be involved in nutrient-dependent mTORC1 translocation to lysosomes. For instance, glucose and glutamine were shown to control the functional assembly and lysosomal localisation of mTORC1 in parallel to Rags via a multiprotein complex TTT-RUVBL1/2 (Kim, Hoffman et al. 2013). Another study identified VPS34 and Phospholipase D, as Rag-independent regulators of amino acid-dependent mTORC1 activation on the lysosomal membrane (Xu, Salloum et al. 2011; Yoon, Du et al. 2011). In addition, Oshiro et al. found that amino-acid mediated activation of mTORC1 did not depend on GTP-loading of Rags, thus suggesting Rag-independent mechanisms of mTORC1 activation (Oshiro, Rapley et al. 2014). That being said, it is important to note, that the Rag-mTORC1 axis is present in other model organisms, such as the fruit fly *Drosophila melanogaster* and baker's yeast *Saccharomyces cerevisiae*, representing an evolutionary conserved mechanism (Kim, Goraksha-Hicks et al. 2008; Sancak, Peterson et al. 2008; Binda, Peli-Gulli et al. 2009; Sancak, Bar-Peled et al. 2010; Gong, Li et al. 2011; Panchaud, Peli-Gulli et al. 2013; Panchaud, Peli-Gulli et al. 2013).

7.3. Autophagy pathway: mechanisms and regulation

Shortage of nutrients results in upregulation of catabolic pathways. Autophagy (from the Greek "self-eating") is one of the most studied catabolic processes in eukaryotic cells. Autophagy was discovered by electron microscopy in 1950-s (Novikoff, Beaufay et al. 1956; Clark 1957; Novikoff 1959) and this morphological approach has remained a predominant method to study this process for several decades (Eskelinen, Reggiori et al. 2011). On the morphological level, autophagy starts by forming a double membrane phagophore (or isolation membrane) that expands and engulfs cytoplasmic components, and finally forms a closed compartment – the autophagosome. Autophagosomes fuse with other autophagosomes and subsequently – with endosomes and lysosomes, to form so called "autolysosomes". In autolysosomes numerous catabolic enzymes degrade the cytoplasmic components that were captured by autophagosomes (Lamb, Yoshimori et al. 2013).

Numerous studies have established autophagy as a major cellular pathway involved in overcoming stress conditions, such as nutrient deprivation (Kuma and Mizushima 2010). However, nutrient-repleted cells also display a certain level of autophagy – so called "basal autophagy". Basal autophagy eliminates damaged or excess proteins and organelles, thus fulfilling housekeeping functions. Basal autophagy is important for maintenance of various organs such as brain, liver and heart (Komatsu, Waguri et al. 2005; Hara, Nakamura et al. 2006; Nakai, Yamaguchi et al. 2007; Kuma and Mizushima 2010; Mizushima and Komatsu 2011).

7.3.1 Molecular mechanisms of autophagy

The molecular mechanisms of autophagy remained unknown till 1990-s, when extensive genetic studies in *S. cerevisiae*, performed by the laboratories of Yoshinori Ohsumi, Michael Thumm and Daniel Klionsky, resulted in the identification of the large (more than 30 members) ATG family of genes involved in this pathway (Takeshige, Baba et al. 1992; Tsukada and Ohsumi 1993; Thumm, Egner et al. 1994; Harding, Hefner-Gravink et al. 1996; Schlumpberger, Schaeffeler et al. 1997). The rapid progress in understanding autophagic mechanisms in yeast had greatly facilitated similar studies in mammalian models, as the majority of ATG proteins are conserved in mammals (Mizushima, Sugita et al. 1998; Kabeya, Mizushima et al. 2000; Mizushima, Yamamoto et al. 2004). Several functional modules of proteins have been found in the autophagic machinery, including:

a) The ULK/Atg1 complex, in which the Serine/threonine-protein kinase ULK1 plays a key role in the induction of autophagy under nutrient starvation conditions;

b) The type III phosphatidylinositol kinase VPS34/Beclin 1 complex that is crucial in early stages of autophagy;

c) Two ubiquitin-like conjugation systems Atg12–Atg5 and microtubule-associated protein 1 light chain 3 (LC3), which are responsible for the formation of autophagosomes.

The schematic overview of these key players in autophagy is shown on **Figure I4**.

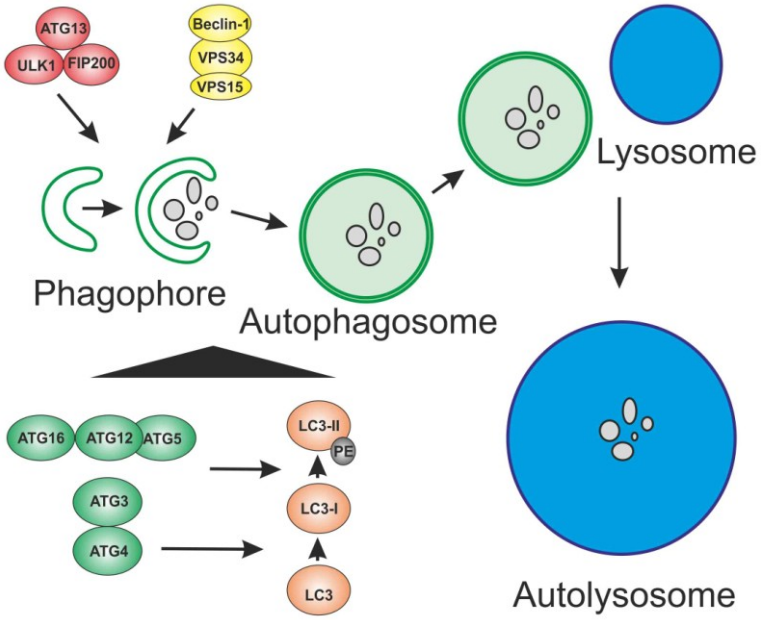

Figure I4. An overview of the autophagic machinery

The ULK/Atg1 complex

Unc-51 like kinase-1 (ULK1), a mammalian homolog of yeast ATG1 was identified as a key autophagy regulator in a siRNA screen, performed by the laboratory of Sharon Tooze. They found that siRNA-mediated knockdown of ULK1 was sufficient to block starvation-induced autophagy in HEK293 cells (Chan, Kir et al. 2007). Subsequent work revealed other members of the ULK complex, including ATG13, ATG101 and RB1CC1 (also known as FIP200) (Ganley, Lam du et al. 2009; Hosokawa, Hara et al. 2009; Jung, Jun et al. 2009). Both ATG13 and RB1CC1 are phosphorylated by ULK1 (Chan, Kir et al. 2007). Interestingly, mammals have another homolog of ATG1 – ULK2; and ULK1 and ULK2 are functionally redundant in mice (McAlpine, Williamson et al. 2013). The ULK complex is required for initial stages of starvation-induced autophagy. The exact molecular mechanisms remain, however, obscure. One interesting link between ULK and other autophagy players was recently found by the laboratory of Kun-Liang Guan. They identified Beclin 1, an important regulator of autophagy (see below), as a substrate of ULK1, and found that phosphorylation of Beclin 1 by ULK1 is

necessary for full induction of autophagy in response to amino acid deprivation (Russell, Tian et al. 2013).

The VPS34/Beclin 1 complex

The type III phosphatidylinositol-3-OH kinase (PI(3)K) complex consists of several members, including VPS34, VPS15 (p150), Beclin 1, Rubicon and ATG14 (Kihara, Kabeya et al. 2001; Zhong, Wang et al. 2009). Upon activation, the PI(3)K complex produces a pool of phosphatidylinositol-3-phosphate (PtdIns(3)P), which recruits its effectors such as WIPI2 (Atg18) to promote autophagosome formation and maturation (Polson, de Lartigue et al. 2010).

In spite of the identification of numerous molecular players involved in the initial stages of autophagy, their exact role and place of action is not yet fully understood. Almost every membrane compartment in eukaryotic cell has been suggested as a source for isolation membranes: endoplasmic reticulum, plasma and nuclear membranes, mitochondria and Golgi apparatus (Yamamoto, Masaki et al. 1990; English, Chemali et al. 2009; Hayashi-Nishino, Fujita et al. 2009; Yla-Anttila, Vihinen et al. 2009; Hailey, Rambold et al. 2010; Ravikumar, Moreau et al. 2010; Hamasaki, Furuta et al. 2013). According to the current view, activated ULK and VPS34/Beclin 1 complexes drive the formation and nucleation of isolation membranes from endoplasmic reticulum. Subsequently, the ubiquitin-like conjugation systems is recruited to the expanding isolation membranes (Lamb, Yoshimori et al. 2013).

The ubiquitin-like conjugation systems in autophagy

Two ubiquitin-like conjugation systems, the ATG5-ATG12 and the light chain-3 (LC3)/ATG8 are crucial for the expansion of isolation membranes and formation of

autophagosomes. These systems employ ubiquitin-like (Ubl) proteins (ATG12 and LC3 respectively) and the Ubl conjugation machinery to recruit LC3 to both, isolation membranes and autophagosomes.

In the Atg5-Atg12 system the E1-like activating enzyme ATG7 and the E2-like conjugating enzyme ATG10 catalyze the covalent binding of ubiquitin-like protein Atg12 to an internal Lysine residue in Atg5 (Mizushima, Sugita et al. 1998; Mizushima, Yamamoto et al. 2001) . Subsequently, Atg5-Atg12 bind to Atg16 (Apg16L), and altogether they are recruited to isolation membranes (Mizushima, Kuma et al. 2003; Fujita, Itoh et al. 2008).

The second Ubl conjugation system mediates the conjugation of Ubl LC3 (homologous to Atg8 in *S. cerevisiae*) to phosphatidylethanolamine. First, the cysteine protease ATG4 cleaves carboxy-terminal residues from LC3 to reveal a carboxy-terminal Glycine, which is subsequently activated by ATG7 (Ichimura, Kirisako et al. 2000; Kirisako, Ichimura et al. 2000). Then, the E2-like conjugating enzyme ATG3 and the Atg12–Atg5–Atg16 complex, that serves as an E3-like enzyme, covalently bind cleaved LC3 (termed LC3-I) through its carboxy-terminal glycine to phosphatidylethanolamine (PE) in isolation membranes to form LC3-II (Ichimura, Kirisako et al. 2000; Fujita, Itoh et al. 2008).

Why is lipidated LC3 required for initial stages of autophagy? This important question is not fully resolved yet. Currently, it is believed that LC3 promotes expansion and completion of autophagosomes, due to its ability to interact with and recruit other proteins to growing autophagosomes, thus defining the cytoplasmic substrates of autophagy and ensuring proper functioning of autophagosomes (Mizushima, Yoshimori et al. 2011; Lamb, Yoshimori et al. 2013). It is also important to note that LC3 is not the only homolog of yeast ATG8 in mammals. The mammalian genome contains at least 8 orthologs of ATG8, that belong to three subfamilies: LC3, γ-aminobutyric acid (GABA) receptor-associated protein (GABARAP) and Golgi-associated ATPase enhancer of 16 kDa (GATE16, also known as

GABARAPL2). While the role of LC3, in particular LC3B, in autophagy is best studied to date, GABARAP/GATE16 members may also be important in distinct steps of autophagy (Kabeya, Mizushima et al. 2004; Weidberg, Shvets et al. 2010; Shpilka, Weidberg et al. 2011).

A substantial number of autophagic players do not belong to the three major groups mentioned above. For instance, the transmembrane protein ATG9 is required for initial steps of autophagy. In particular, the trafficking of ATG9 from juxtanuclear position in the Golgi to peripheral endosomes upon induction of autophagy is important for formation of autophagosomes (Young, Chan et al. 2006). Another important example led to an answer to a long-running question related to mechanisms underlying the latest steps of autophagy. A recent study from the laboratory of Noboru Mizushima identified syntaxin 17, located on the autophagosomal membrane, as a SNARE protein that interacts with SNAP-29 and the endosomal/lysosomal SNARE VAMP8 to mediate fusion of autophagosome to lysosomes (Itakura, Kishi-Itakura et al. 2012).

7.3.2. Regulation of autophagy by mTORC1

As it was mentioned above, mTORC1 is a major suppressor of autophagy. The best known functional link between mTORC1 and autophagy is inhibitory phosphorylation of the ULK complex by mTORC1. It was shown that active mTORC1 directly binds to ULK1 through Raptor and phosphorylates ULK1/ULK2 as well as ATG13 (Ganley, Lam du et al. 2009; Hosokawa, Hara et al. 2009; Jung, Jun et al. 2009; Kim, Kundu et al. 2011; Shang, Chen et al. 2011). Interestingly, mTORC1-mediated phosphorylation of the ULK complex does not disturb its assembly, which is the case in yeast. Therefore, it is possible that phosphorylation of ULK1 by mTORC1 exerts its inhibitory functions by changing ULK localisation, separating it from its autophagic targets (Wong, Puente et al. 2013).

Besides ULK, several other proteins involved in autophagy are controlled by mTORC1. Death-associated protein 1 (DAP1) which was identified as a suppressor of autophagy was shown to be a target of mTORC1, but the exact function of DAP1 in autophagy remains elusive (Koren, Reem et al. 2010). The autophagic protein WIPI2 was found as a potential substrate of mTORC1 in a large phosphoproteome screen (Hsu, Kang et al. 2011). In addition, a recent study from the laboratory of Francesco Cecconi unveiled a new link between mTORC1 and ULK. They found that Beclin 1-interacting protein AMBRA1 promotes ubiquitination of ULK complex on Lysine 63 by E3-ligase TRAF6, that results in enhanced stability and activity of the ULK complex. They showed that mTORC1 inhibits AMBRA1, thus impairing ubiquitination of ULK complex (Nazio, Strappazzon et al. 2013).

Several signalling networks involved in the regulation of autophagy converge into mTORC1. For example, AMP-activated kinase (AMPK) serves as a low energy sensor that counteracts mTORC1. AMPK was shown to inhibit mTORC1 by phosphorylating Raptor (Gwinn, Shackelford et al. 2008). In addition, AMPK phosphorylates and activates ULK1, which is prevented by mTORC1-mediated ULK1 phosphorylation (Kim, Kundu et al. 2011).

Conclusively, it is important to note that our current knowledge of autophagy is far from being complete. The overview of basic mechanisms shown here does not stand as a dogma. Importantly, certain autophagic pathways do not rely on the VPS34/Beclin 1 complex (Scarlatti, Maffei et al. 2008), on ULK (Cheong, Lindsten et al. 2011) or even on LC3 (Nishida, Arakawa et al. 2009) and mTORC1 (Williams, Sarkar et al. 2008).

7.4. Pancreatic β cells sense nutrient availability to control whole body metabolism

On the organismal level, the control of metabolism is achieved through the coordinated action of hormones produced by the endocrine system. In mammals, nutrient availability is sensed by pancreatic β cells that produce and secrete insulin – the central anabolic hormone. In a fed state, glucose together with other nutrients (such as amino acids) derived from the food, induce secretion of insulin by β cells. Secreted insulin increases glucose uptake in the body and promotes anabolic processes in tissues. The mechanisms of β cell function, in particular, insulin production and secretion have been a subject of extensive studies for many decades, as the failure of β cells results in a severe metabolic disorder – Diabetes mellitus (Ashcroft and Rorsman 2012).

Insulin is synthesized as a precursor preproinsulin on the ribosomes of the Rough Endoplasmic Reticulum (RER), and is cleaved to proinsulin during its translocation into the lumen of RER. Subsequently, proinsulin molecules pass through RER and Golgi to the Trans-Golgi Network (TGN) to be packed inside of the special vesicles, so-called insulin Secretory Granules (SGs). SGs serve as a compartment where maturation of proinsulin to insulin occurs through coordinated activity of endopeptidases. Exocytosis of SGs upon stimulation results in insulin release (Goodge and Hutton 2000; Steiner 2011). The main steps of insulin biosynthesis are shown on a **Figure I5**.

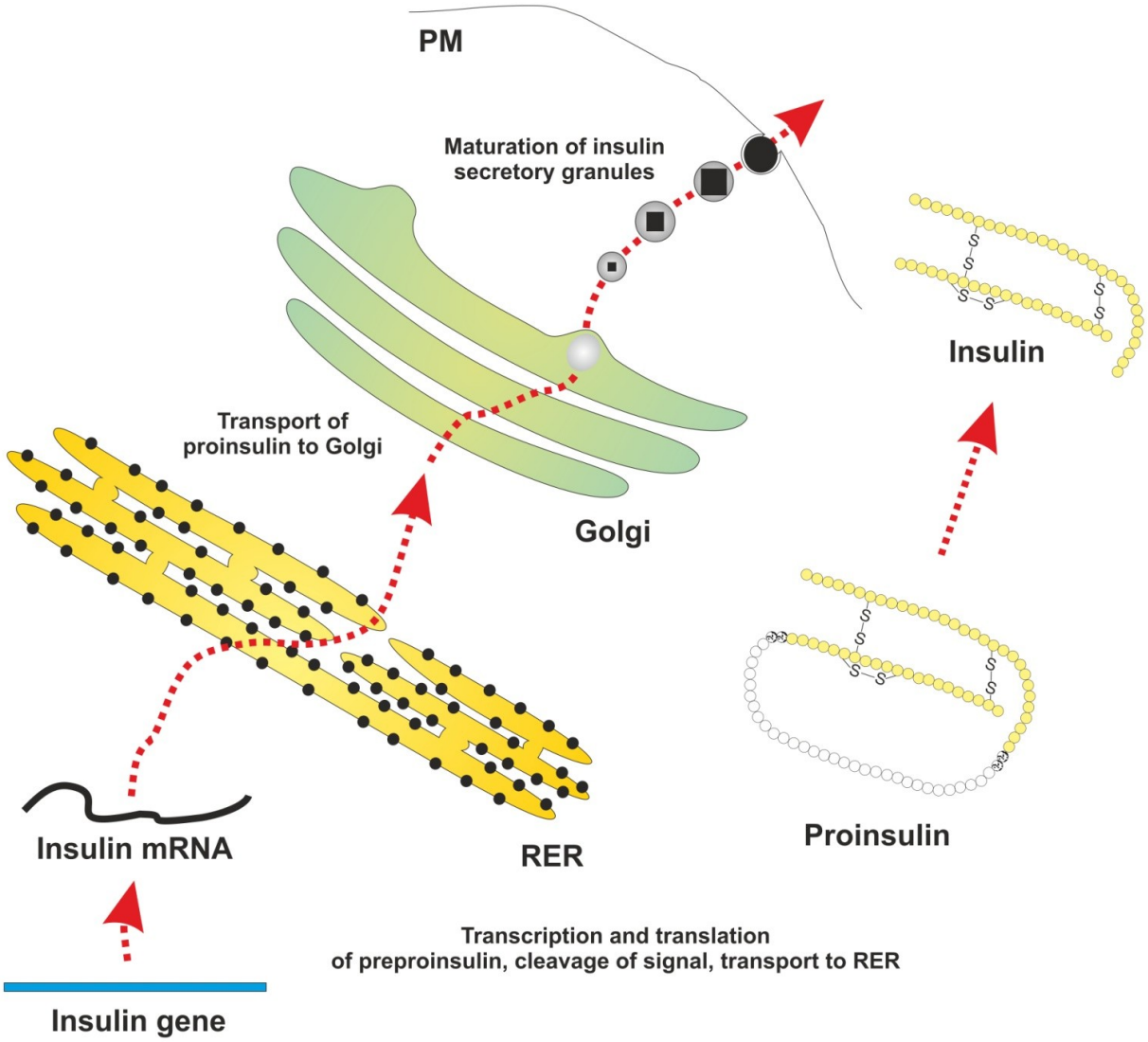

Figure I5. An overview of the insulin biosynthesis. RER: Rough Endoplasmic Reticulum. PM: plasma membrane. Schematic representations of human proinsulin and insulin molecules are shown on the right

While the core machinery underlying insulin biosynthesis and secretion is relatively well studied, the signalling cascades involved in its regulation are less well understood. A series of studies, performed in our lab unveiled a novel signalling axis that controls secretion of

insulin. We identified Protein Kinase D1 (PKD1) as a key regulator of early steps of SGs biogenesis. PKD1 phosphorylates BAR domain-containing protein Arfaptin-1 at Serine 132, which is required for timely scission of SGs at the TGN (Gehart, Goginashvili et al. 2012). Importantly, upregulation of PKD1 activity *in vivo* results in a marked increase in insulin secretion and protects β cells in a model of diabetes (Sumara, Formentini et al. 2009).

How do nutrients promote insulin release? According to the most accepted model, metabolic activity in β cells drives secretion of insulin (Prentki, Matschinsky et al. 2013; Rorsman and Braun 2013). The activation of metabolism due to uptake of nutrients leads to the raise of cellular ATP/ADP ratio, which results in the closure of ATP-sensitive potassium channels. Due to the latter event, rapid depolarisation of cell membrane occurs, thus promoting opening of calcium channels and subsequent calcium influx. Subsequently, increased cellular calcium triggers exocytosis of SGs (Prentki, Matschinsky et al. 2013). In spite of the fact that some of the distal steps of insulin secretion events had been recently debated (Szollosi, Nenquin et al. 2007; Szollosi, Nenquin et al. 2007; Ravier, Nenquin et al. 2009), the consensus is reached on the tight link between β cell metabolism and secretion of insulin (Ashcroft and Rorsman 2012; Prentki, Matschinsky et al. 2013; Rorsman and Braun 2013).

While enormous number of studies concentrated on the response of β cells to nutrient uptake, surprisingly little is known about the β cells' behaviour during fasting, when secretion of insulin is kept at a very low level. Moreover, the role of autophagy in the adaptation of β cells to shortage of nutrients is not entirely clear. Although experiments in starved pancreatic islets and β cell lines suggested the involvement of autophagy in the nutrient starvation response, especially after long-term starvation, studies performed in mice did not reveal an increase in autophagy under starvation conditions (Ebato, Uchida et al. 2008; Fujitani, Ueno et al. 2010)**.** Only prolonged starvation of mice for 24 hours induced autophagy in β cells (Fujimoto,

Hanson et al. 2009). Conclusively, the cellular mechanism underlying the nutrient starvation response in pancreatic β cells currently remains elusive and is the subject of my thesis.

8. Materials and Methods

The text and figures shown in chapters 'Materials and Methods' and 'Results and Discussion' have been partially taken from the following manuscript:

Goginashvili A., Erbs E., Kessler P., Pasquier A., Schieber N., Cinque L., Krupina K., Morvan J., Sumara I., Schwab Y., Settembre C., Ricci R. PKD links Golgi to nutrient starvation response in pancreatic β cells. Science (in revision).

8.1. Materials

Reagents were obtained from the following sources: HRP-labeled anti-mouse and anti-rabbit secondary antibodies from IGBMC; antibodies to phospho-S757 ULK1, ULK1, phosphoT389 S6K1, S6K1, mTOR from Cell Signaling Technology; antibody to LC3B (2G6) from nanoTools; antibody to Lamp1 (Ly1C6) from Cayman Chemical; antibody to Proinsulin (C-Peptide I) from Serotec; antibody to Giantin from Enzo Life Sciences; antibody to Green Fluorescent Protein from Fisher Scientific; antibody to PKD1 (c-20) from Santa Cruz; Gö 6976, type V Collagenase solution, Histopaque 1119, Pepstatin A, E64D, amino acids, Bafilomycin A1, puromycin, antibodies against GAPDH and insulin, non-silencing small hairpin RNAs, small hairpin RNAs against PKD1 from Sigma Aldrich; Vectashield from Vector Laboratories; Mowiol from Calbiochem; cOmplete Protease Inhibitor Cocktail Tablets from Roche; Rapamycin, Torin 1 and CID755673 from Tocris Biosciences; 4',6-diamidino-2-phenylindole (DAPI), Image-iT® FX signal enhancer and Alexa -488, -568 and 647 conjugated secondary antibodies from Life Technologies; DyLight 405-conjugated secondary antibody from Jackson ImmunoResearch Laboratories; Alexa-488 conjugated

secondary antibody pGolgi-CFP (Addgene: 14873, deposited by Alexandra Newton, University of California at San Diego), ptfLC3 (Addgene: 21074, deposited by Tamotsu Yoshimori, Osaka University), pEGFP-LC3 (Addgene: 21073, deposited by Tamotsu Yoshimori), Lamp1-RFP (Addgene: 1817, deposited by Walther Mothes, Yale University) were obtained from Addgene. G-PKDrep-live (Eisler, Fuchs et al. 2012) was kindly provided by Angelika Hausser (University of Stuttgart). Phogrin-GFP (Pouli, Emmanouilidou et al. 1998) was kindly provided by Guy Rutter (Imperial College London). An antibody against Phogrin was a generous gift from John Hutton (University of Colorado).

8.2. Mice

p38δ$^{-/-}$ mice were described previously (Sumara, Formentini et al. 2009). GFP-LC3 transgenic mice were generated by Noboru Mizushima (Mizushima, Yamamoto et al. 2004) and distributed by the RIKEN Bio-Resource Center (Japan). Maintenance and animal experimentation were in accordance with the Committee on Animal Care at Azienda Ospedaliera "Antonio Cardarelli", Italy or the veterinarian services, Strasbourg, France in compliance with the European legislation on care and use of laboratory animals.

8.3. Cell lines and transfections

INS1 cells were maintained in RPMI 1640 supplemented with 10% FCS, 10 mM Hepes, 1 mM PyrNa. HEK293 and INS1 cells were transfected by using Amaxa Nucleofector (Lonza) according to the manufacturer's protocol. PKD1 was knocked down by lentiviral transduction

of small hairpin constructs in pLKO.1 puro (Sigma Aldrich) against PKD1. The cells were selected by addition of 0.5 ug/ml Puromycin (Sigma Aldrich).

8.4. Nutrient deprivation

For nutrient deprivation almost confluent INS1 cells, HEK293 cells or intact primary islets were incubated in Krebs-Ringer Bicarbonate Buffer (KRB) (136 mM NaCl, 4.7 mM KCl, 1.2 mM MgS04, 1 mM CaCl2, 1.2 mM KH2PO4, 5 mM NaHCO3, 10 mM HEPES (pH 7.4)) , supplemented with 0.5% BSA (designated as "no Glc/FCS") or with 5.5 mM or 11 mM glucose ("no AA/FCS") and compared to full media ("GC"). For an experiment shown in Fig 4H, intact primary islets were incubated in KRB, supplemented with 0.5% BSA and 2.8 mM glucose. Inhibitors of lysosomal proteases Pepstatin A (10 μg/ml) and E64D (10 μg/ml) were used in experiments, shown in Fig R2C and R2D.

To address nutrient starvation response in β cells *in vivo* (Fig R1E) mice were pre-fasted for 24 h, then fed for 2 h (9AM–11AM) (designated as "Fed") and either sacrificed or re-fasted for 4h (designated as "Fasted") prior sacrifice.

8.5. Immunofluorescence

INS1 cells were plated on 9-15 mm glass coverslips (Menzel-Glaser) in 24-well tissue culture plates and allowed to grow for 24 hours. In the end of experiment the cells were washed once with PBS and fixed for 20 minutes with 4% paraformaldehyde (PFA) in PBS at room temperature. The coverslips were rinsed twice with PBS and permeabilized with 0.1% Triton X-100 in PBS for 5 minutes. After rinsing three times with PBS, the coverslips were blocked

by Image-iT FX signal enhancer (Life Technologies), rinsed once with PBS and incubated for 30 minutes in blocking buffer (3% BSA in PBS). Coverslips were subsequently incubated with primary antibodies in blocking buffer for 1 hour at room temperature or overnight at 4°C, rinsed three times with PBS and incubated with secondary antibodies, diluted in blocking buffer, for one hour at room temperature in the dark. After incubation coverslips were rinsed three times with PBS (with DAPI added in the 2nd wash step, where indicated) and mounted on glass slides using Vectashield (Vector Laboratories) or Mowiol (Calbiochem) and imaged with a 100X or 63X objective using epifluorescence microscope or confocal microscope Leica Spinning Disk Andor/Yokogawa.

8.6. Histochemistry

Pancreata were fixed by intracardiac perfusion with PFA 4% in PBS. Tissues were postfixed overnight at 4°C in the same solution, cryoprotected in 30% sucrose in PBS solution, embedded in Cryomatrix (Thermo scientific) and kept at -80° C. Pancreas sections were cut with a cryostat (CM3050, LEICA) and mounted on Superfrost Ultra Plus slides (Menzel-Glaser). 10 µm cryosections were incubated for 2 hours at room temperature in the blocking solution (PBS/ 5% Normal Goat Serum /0.3% TritonX100), then left overnight at 4°C, in a wet chamber, with a mouse monoclonal primary antibody raised against Insulin (I2018, Sigma Aldrich) and a rabbit polyclonal primary antibody raised against (GFP,A-6455, Fisher scientific) diluted in the blocking solution. After 3 washes in PBS, the sections were blocked for 15 min at room temperature in the blocking solution and incubated for 2 hours at room temperature, in wet chamber, with an Alexa-568 conjugated Goat Anti Mouse secondary antibody (A11031, Molecular Probes) and an Alexa-488 conjugated Goat Anti Rabbit secondary antibody (A11034, Fisher scientific) diluted in the blocking solution.

After 3 washes in PBS, 1 wash in H2O and 1 brief wash in ethanol 70%, the slides were dried and mounted in Mowiol (Calbiochem) containing DAPI (0.5µM). Images were taken using confocal microscope Leica Spinning Disk Andor/Yokogawa.

8.7. Isolation of pancreatic islets

Mice were anesthetized by a mix of 20% ketamine-10% xylasine. Islets were isolated by perifusion of 5ml of type V Collagenase (Sigma Aldrich) solution and separation through a Histopaque 1119 (Sigma Aldrich) gradient. Islets were kept in RPMI 1640 supplemented with 10%FCS, 10mM Hepes, 1mM PyrNa and penicillin/streptomycin.

8.8. Transmission electron microscopy (TEM)

For TEM, cells and primary islets were first fixed in 0.05% malachite green, 2.5% glutaraldehyde, 0.1 M sodium cacodylate buffer, postfixed in 0.8% K3Fe(CN)6, 1.0% OsO K3Fe(CN)6 and stained with 1% tannic acid and 0,5% uranyl acetate. The samples were then dehydrated in graded ethanol solutions and embedded in Epon (Ladd Research Industries). Ultrathin sections (50-60 nm) were examined under a Philips CM12 80 kV electron microscope equipped with an ORIUS SC1000 CCD camera.

Quantitative analyses of autophagic compartments of INS-1 cells and primary islets have been assessed by TEM as described (Yla-Anttila, Vihinen et al. 2009). Briefly, the areas of cytoplasm and Golgi were evaluated by stereological approach using x5600 magnification with ImageJ-based open-source Fiji software package. The numbers of autophagic compartments were quantified using x15000 magnification. Data from 3 independent

experiments were expressed as mean ± SEM. The numbers of granule-containing lysosomes (GCLs) in Golgi area were counted for 30 cells from 3 independent experiments using x19500 magnification. The data were expressed as mean ± SEM. All quantitative analyses relied on systematic uniform random sampling.

8.9. Correlative Light and Electron Microscopy (CLEM)

CLEM was performed as described (Lenormand, Spiegelhalter et al. 2013). In brief, INS1 cells were cultured on laser micro-patterned Aclar supports. In the end of experiment the cells were fixed in PFA 4%, Glutaraldehyde 0,5% in sodium cacodylate 0,1M for 20 minutes at room temperature, followed by incubation in sodium cacodylate 0,1M. Cells of interest were selected, precisely located and imaged by fluorescence confocal microscopy using Leica Spinning Disk Andor/Yokogawa microscope. The samples were then processed exactly as for TEM.

8.10. Ratiometric measurements and analysis

INS1 cells, transiently transfected with G-PKDrep-live were plated on glass bottom Petri dishes (ASAHI GLASS Co, Iwaki) and allowed to grow for 24 hours. Cells were incubated in Phenol Red-free RPMI 1640 supplemented with 10%FCS, 10mM Hepes, 1mM PyrNa and penicillin and streptomycin 12 hours prior imaging.

Ratiometric measurements were performed on a Leica TCS SP8 AOBS inverted confocal microscope, with a Leica HC PL APO CS2 63x/1.2 water immersion objective. Fluorescence excitation was achieved using an Argon Laser (458 nm) and two Leica HyD detectors were

used to simultaneously record the emission of the donor (CFP) and acceptor (YFP) signals between 467-497 nm and 535-565 nm respectively. A “cube & box” system from Life Imaging Services was used to keep both cells and microscope under 37°C and the Leica Adaptive Focus Control (AFC) was engaged to maintain the focus during the time-lapse imaging. Multi-position imaging was performed to record cells automatically, providing a time-resolution of 1 image / 30 s per cell.

YFP/CFP ratio from 30 cells from 3 independent experiments was calculated cell by cell and time by time using a macro developed on ImageJ-based open-source Fiji software package. Ratios were normalized and represented on figure 4F as mean ± s.e.m.

8.11. Metabolic labeling with [35S] methionine

Proinsulin biosynthesis and conversion of proinsulin to insulin were analyzed by (pro)insulin immunoprecipitation of [35S] methionine-radiolabeled INS-1 lysates as described (Wicksteed, Herbert et al. 2001). Briefly, to address proinsulin biosynthesis INS 1 cells were incubated in KRB with 2.8 mM glucose for 1 hour, followed by incubation in KRB either with 2.8 mM or 22 mM glucose. The last 20 minutes of incubation was carried out in the presence of 250 µCi/ml [35S]-methionine. Then cells were collected, washed, lysed in IP Buffer (50 mM Tris (pH 7.5), 50 mM NaCl, 0.5% Triton X-100, 0.5% NP40 substitute, 5 mM EGTA, 5 mM EDTA, 20 mM NaF, 25 mM beta-glycerophosphate, 1 mM PMSF, 0.1 mM NaVO3, 1x complete protease inhibitor (Roche)) and subsequently immunoprecipitated for (pro)insulin with Anti-Insulin antibody (I8510, Sigma Aldrich). Immunoprecipitated 35S-labeled (pro)insulin was then subjected to SDS-PAGE and visualized by phosphoimager.

In pulse-chase experiments, INS 1 cells were incubated in KRB with 25 mM glucose for 1 hour, the last 30 minutes of incubation were carried out in the presence of 250 µCi/ml [35S]-

methionine (pulse). After pulse, cells were washed and then chased for 0, 3 or 6 hours in KRB with 5.5 mM glucose. At each chase time point, cells were collected, washed, lysed in IP Buffer and subsequently immunoprecipitated for (pro)insulin with Anti-Insulin antibody (I8510, Sigma). Immunoprecipitated [35S]-labeled (pro)insulin was then subjected to SDS-PAGE and visualized by phosphoimager.

8.12. Insulin secretion

Insulin secretion was performed as previously described (Sumara, Formentini et al. 2009). Briefly, INS-1 cells were incubated for 30 min in KRB supplemented with 0.5% BSA, and 2.8 mM glucose. Subsequently, INS-1 cells were incubated for 1 hourr in the same buffer in presence of Rapamycin (100 nM) or DMSO. After 1 hourr the supernatant was collected and the remaining cells were lysed in IP Buffer. The insulin secretion in the supernatants was measured using an Ultra Sensitive Mouse Insulin ELISA Kit (ALPCO Diagnostics). Data were normalized to non-treated control cells.

8.13. Cell lysis

Cells were rinsed once with ice-cold PBS and lysed in ice-cold lysis buffer (50 mM Tris (pH 7.5), 50 mM NaCl, 0.5% Triton X-100, 0.5% NP40 substitute, 5 mM EGTA, 5 mM EDTA, 20 mM NaF, 25 mM beta-glycerophosphate, 1 mM PMSF, 0.1 mM NaVO3, 1x complete protease inhibitor (Roche)). The soluble fractions of cell lysates were isolated by centrifugation at 12800 rpm for 10 minutes.

8.14. Molecular cloning

Cloning of cytoplasmic tail (amino acids 625-1004) of Phogrin into pGex-4T1 in frame with GST was performed by PCR amplification of this region in Phogrin-GFP, which introduced restriction sites for restriction enzymes EcoRI and SalI, used for following restriction and ligation. Primers used for cloning were: 5'CCCGAATTCGCCTACTGCCTCCGC3' (forward) and 5'CCGTCGACCTACTGGGGAAGGGC-C3' (reverse). Restriction and ligation were performed according to standard procedures using restriction enzymes and ligase from New England Biolabs and Fermentas.

8.15. Generation of recombinant proteins

pGex-4T1 vector was used for expression of GST-tagged proteins in BL21DE3 strain. At log phase of growth (OD600 0.5), protein expression was induced by addition of isopropyl-β-D-thiogalactopyranosid (IPTG) (0.4 mM) at 25 °C for 4 hours. Then, cells were resuspended in 15 ml of NETN buffer containing complete protease inhibitor (Roche) and lyzed by addition of Lysozyme (100 ug/ml), followed by 30 minutes of incubation on ice and subsequent sonication. The lysates were cleared by centrifugation (12000g, 15 minutes, 4°C). Next, 500 µl of glutathione (GSH)-bound beads were added to the supernatant, followed by mixing by rotation for 2 hours at 4°C. The beads were collected and washed 4 times with NETN. The GST-tagged proteins were eluted twice with reduced Glutathione (Sigma Aldrich) (15 mM in Tris (pH 9)) for 15 minutes. Eluates were dialysed and stored at -80°C in PBS substituted with 20% Glycerol.

8.16. In-vitro kinase assay

Recombinant GST-tagged PhogrinCyto and hArfaptin-1 were incubated with recombinant PKD1 (GenWay) in Kinase Buffer (20 mM MgCl, 25 mM Hepes pH 7.6, 1 mM DTT) supplemented with 20 mM ATP and 5 µCi [gamma-32P] ATP for 30 minutes at 30°C in the presence of absence of 50 µM Gö6976 (Sigma Aldrich). Next, proteins were separated by SDS-PAGE and blotted on PVDF membranes. Autoradiography was visualized by phosphoimager.

8.17. Mammalian lentiviral shRNAs

shPKD1_1

CCGGGAAACACGAAACTTGTTATTGCTCGAGCAATAACAAGTTTCGTGTTTCTTTTTTG

shPKD1_2

CCGGCCCACGCTCTCTTTGTTCATTCTCGAGAATGAACAAAGAGAGCGTGGGTTTTT

8.18. Statistical analyses

The statistical significance of the differences between two groups was investigated by unpaired t test or by Mann - Whitney U-test. For comparison of more than two groups one-way ANOVA followed by Tukey HSD test was used. The statistical analysis was performed using GraphPad Prism software (GraphPad Software Inc.).

9. Results and Discussion

Proper nutrient sensing is crucial for multicellular organisms. In mammals upon feeding, the pancreatic β cells mainly sense increasing glucose levels and secrete insulin that acts to induce anabolic pathways in different organs. Inversely, the β cells decrease insulin secretion to suppress these anabolic reactions upon low glucose levels during fasting (Rorsman and Braun 2013). As known for many eukaryotic cells, nutrient deprivation is expected to induce autophagy. During autophagy, cellular components are sequestered into double-membrane autophagosomes, which subsequently fuse with lysosomes (autolysosomes), where degradation occurs. Resulting catabolites maintain cells metabolically active, ensuring cell survival (Shintani and Klionsky 2004; Rabinowitz and White 2010; Lamb, Yoshimori et al. 2013). However, the role of autophagy in the nutrient starvation response in pancreatic β cells remains elusive (Ebato, Uchida et al. 2008; Fujimoto, Hanson et al. 2009; Fujitani, Ueno et al. 2010) and is addressed in my study.

9.1. Nutrient depletion suppresses autophagy in β cells

Firstly, I wanted to address the role of autophagy in the nutrient starvation response of β cells. To this aim, I used LC3B localisation as the readout of autophagy. As mentioned above, induction of autophagy is marked by incorporation of LC3B into membranes of autophagosomes that appear as punctate structures (Tanida, Ueno et al. 2004). INS1 cells (β cell line derived from insulinoma of rats) that transiently expressed LC3B tagged with GFP (LC3B-GFP) contained 35.62 ± 2.87 (hereafter, shown as mean ± s. e. m.) LC3B-GFP puncta under nutrient-rich conditions, indicating basal autophagy. Unexpectedly, INS1 cells deprived

of serum and amino acids (AA) for 2 or 6 hours contained 14.5 ± 1.14 and 18.56 ± 1.51 LC3B-GFP puncta, respectively. Similarly, depletion of INS1 cells from serum and glucose (Glc) for 2 or 6 hours drastically decreased LC3B-GFP puncta to 8.08 ± 1.01 and 13.08 ± 1.51, respectively (Fig. R1A). Deprivation from serum alone did not change the amount of LC3B-GFP puncta (Supplementary fig. R1). In strong contrast and as previously reported (Kabeya, Mizushima et al. 2000), starved human embryonic kidney 293 (HEK-293) cells displayed markedly increased LC3B-GFP puncta as compared to non-starved cells (Supplementary fig. R2).

Reduction in LC3B-GFP puncta may be explained by two scenarios. First, it is possible that autophagy is decreased upon nutrient starvation. Alternatively, decreased number of LC3B-GFP puncta at a particular time point may indicate high autophagy with rapid lysosomal disposal of LC3B-GFP, resulting in disappearance of the GFP signal. To distinguish between these two possibilities, I measured autophagic flux with the help of RFP-GFP tandem fluorescence-tagged LC3 (ptfLC3). In ptfLC3 expressing cells, the GFP tag is acid-sensitive and the RFP tag is acid-insensitive, allowing for discrimination between yellow fluorescent autophagosomes and red fluorescent autolysosomes (Kimura, Noda et al. 2007). Time-lapse fluorescent microscopy of INS1 cells transfected with ptf-LC3 deprived from serum and AA or Glc revealed rapid reduction in the number of RFP-GFP and no increase in RFP-only puncta (Fig. R1B and Supplementary fig. R3). To confirm the autophagic origin of RFP-GFP and RFP-only puncta, I performed Correlative Light and Electron Microscopy (CLEM). CLEM corroborated reduced numbers of autophagosomes and unchanged numbers of autolysosomes in AA/serum-depleted INS1 as compared to non-starved cells (Fig. R1C). Quantitative EM (QEM) confirmed this observation in β cells of AA/serum-deprived murine primary islets, revealing 12.43 ± 1.73 and 3.6 ± 0.6 autophagic compartments

(autophagosomes and autolysosomes) per 100 μm^2 under nutrient-rich conditions and upon AA/serum deprivation, respectively. (Supplementary fig. R4).

To measure endogenous autophagic flux, I used Bafilomycin A1 (Baf A1) that blocks autolysosomal degradation of LC3B (Yamamoto, Tagawa et al. 1998). Treatment with Baf A1 led to a decreased accumulation of lipidated autophagosomal LC3B (LC3B-II) in AA/serum-starved as compared to non-starved INS1 cells, indicating decreased autophagic flux upon AA deprivation (Fig. R1D). Observed changes of autophagy were confirmed *in vivo* comparing β cells in pancreatic islets derived from fed and fasted LC3B-GFP expressing mice (Mizushima, Yamamoto et al. 2004). β cells of fed and fasted mice contained 33.08 ± 2.20 and 21.53 ± 1.75 LC3B-GFP puncta per 1600 μm^2, respectively (Fig. R1E). Collectively, the obtained data suggest that autophagy is not a major mechanism to overcome nutrient deprivation in β cells.

9.2. Nutrient depletion induces SINGD in β cells

The findings shown above strongly suggest that β cells utilize a distinct mechanism to adapt to changes in nutrient availability. Besides autophagy, selective degradation of secretory granules (SGs) by their direct fusion with the lysosomes in the process called "crinophagy", could be involved in β cells response to starvation (Smith and Farquhar 1966; Sandberg and Borg 2006). To analyze crinophagy, I assessed cellular localization of lysosomal Lamp1 and SG protein Phogrin. Phogrin- and Lamp1-positive puncta in INS1 cells increased from 14.6 ± 1.18 under growing conditions to 37.6 ± 1.98 upon AA and serum withdrawal for 2 hours (Fig. 2A). Lamp1 and Phogrin preferentially co-localized in proximity to the Golgi (Fig. R2A). QEM of AA/serum starved INS1 cells corroborated this finding, revealing abundant lysosomes containing electron-dense SGs in proximity of the Golgi (Supplementary fig. R5).

CLEM confirmed that the latter structures corresponded to puncta of Lamp1 and Phogrin colocalization (Fig. R2B). In addition, treatment of AA/serum-deprived cells with lysosomal protease inhibitors increased Lamp1 and Phogrin co-localization in comparison with non-starved cells (Fig R2C), confirming lysosomal degradation of SGs.

SGs are generated at the trans-Golgi network (TGN). I thus wondered whether nascent granules are specifically targeted to lysosomes. Readily formed SGs contain proinsulin, which is subsequently converted into insulin (Steiner, Cunningham et al. 1967). 6 hour depletion from AA and serum led to an almost complete loss of proinsulin (Fig. R2D). Decrease of proinsulin was partially restored by lysosomal protease inhibitors (Fig R2D) suggesting that nutrient deprivation leads to lysosomal degradation of *de novo* synthesized SGs in pancreatic β cells. I confirmed aforementioned findings *ex vivo*, by performing QEM of nutrient-deprived primary murine islets. QEM revealed abundant lysosomes that contained electron-dense SGs in the Golgi areas of AA/serum–starved islets (Fig. R2E and quantification in Supplementary fig. R6). Overall, these data suggest that β cells mainly employ Starvation-Induced Nascent Granule Degradation (SINGD) instead of autophagy to counteract shortage of nutrients.

9.3. SINGD suppresses autophagy in an mTOR-dependent manner

Lysosomal AAs derived from degraded proteins induce translocation of mammalian (or mechanistic) Target Of Rapamycin Complex 1 (mTORC1) to lysosomal membranes (Sancak, Peterson et al. 2008; Zoncu, Bar-Peled et al. 2011), mTORC1 activation (Sancak, Peterson et al. 2008; Zoncu, Bar-Peled et al. 2011) and subsequent suppression of autophagy (Yu, McPhee et al. 2010; Betz and Hall 2013; Kim, Buel et al. 2013). Do lysosomes involved in SINGD suppress autophagy through mTORC1? Strikingly, mTOR inhibitors rapamycin and

torin 1 increased the number of LC3B-GFP puncta in AA/serum-depleted INS1 cells to 24.25 ± 1.79 and 25.4 ± 2.32, respectively as compared to 11.5 ± 0.97 LC3B-GFP puncta in non-inhibited AA/serum-depleted INS1 cells (Fig. R3A). This indicates that mTORC1 activity is required for suppression of autophagy upon starvation. Moreover, depletion of AA and serum from INS1 cells resulted in translocation of mTOR to Phogrin/Lamp1-positive puncta close to the Golgi area (Fig. R3B). mTORC1 was shown to suppress starvation-induced autophagy through inhibitory phosphorylation of Unc-51-like kinase 1 (ULK1) on Serine 757 (ULK1-S757). Thus, starvation is expected to decrease ULK1-S757 phosphorylation (Kim, Kundu et al. 2011). Western blotting revealed that ULK1-S757 phosphorylation levels remained high in starved as compared to non-starved INS1 cells (Fig. R3C). Importantly, phosphorylation of ULK1-S757 was markedly decreased when mTORC1 was inhibited by rapamycin (Fig. R3C). Interestingly, while under nutrient-rich conditions S757-ULK1 phosphorylation appeared as discrete fluorescent dots throughout the cytoplasm, AA/serum deprivation led to the formation of large bright S757-ULK1 puncta that co-localized with both Lamp1 and Phogrin close to the Golgi (Fig. R3D). Collectively, these data suggest that mTORC1-mediated ULK1-S757 phosphorylation in the SINGD compartment is important for suppression of autophagy. Levels of ULK1-S757 phosphorylation did not increase under starving as compared to growing conditions, suggesting that observed basal autophagy in non-starved cells is largely independent of ULK1-S757 phosphorylation. Phosphorylation of the mTORC1 substrate S6K1 on threonine 389 (T389), involved in regulation of protein translation (Pearson, Dennis et al. 1995), almost completely disappeared during starvation (Fig. R3C). This is in line with a previous report showing that S6K1 phosphorylation requires higher mTOR activity than ULK1 phosphorylation (Kang, Pacold et al. 2013). Altogether, these data suggest that nutrient depletion leads to induction of SINGD that locally activates mTOR to suppress autophagy.

9.4. PKD1 is a key player in SINGD

9.4.1. Inactivation of PKD1 is sufficient to trigger SINGD

How is SINGD controlled? Degradation of nascent SGs in vicinity of the Golgi is likely to rely on molecular mechanisms involved in SG biogenesis. We and others identified Protein Kinase D1 as a key regulator of early steps of insulin SG biogenesis at the TGN (Sumara, Formentini et al. 2009; Gehart, Goginashvili et al. 2012; Cruz-Garcia, Ortega-Bellido et al. 2013). Thus, PKD1 inactivation could have an effect on the turnover of *de novo* formed SGs. Indeed, treatment of INS1 cells with the PKD inhibitor CID 755673 (Sharlow, Giridhar et al. 2008) markedly decreased the amount of proinsulin (Fig. R4A). This decrease in proinsulin content could be due to decreased biosynthesis of proinsulin or because the β cells cannot properly store it. To distinguish between these possibilities, I tested the rates of proinsulin biosynthesis in INS1 cells stably expressing shRNA against PKD1 or control non-silencing shRNA. The biosynthesis of proinsulin was unchanged in the absence of PKD1 as compared to control (Supplementary fig. R7 and R8). However, accumulation of newly formed insulin was markedly decreased in PKD1 knockdown cells, indicating enhanced degradation of *de novo* synthesized insulin (Supplementary fig. R9). QEM analysis of cells lacking PKD1 revealed abundant lysosomes that contained SGs in the Golgi area (Fig. R4B and Supplementary fig. R10). Would inactivation of PKD1 lead to mTOR-dependent suppression of autophagy, as SINGD does? Strikingly, mTOR largely co-localized with lysosomal Lamp1 in cells depleted of PKD1 (Fig. R4C). Moreover, mTOR-mediated ULK1-S757 phosphorylation was markedly increased (Fig. R4D). As in SINGD, autophagic flux was considerably suppressed upon PKD1 knockdown (Fig. R4E).

9.4.2. Nutrients control activity of PKD1

If SINGD is controlled by PKD1, PKD1 activity in the Golgi is likely to be regulated by nutrients.

Catalytically inactive mutants of PKD1 were used to address the localization of this kinase in response to different stimuli (Liljedahl, Maeda et al. 2001; Baron and Malhotra 2002; Hausser, Link et al. 2002). I found that GFP-tagged catalytically inactive K612W mutant of PKD1 (PKD1-K612W-GFP) was localised to Golgi and plasma membrane under growing conditions in INS1 cells. Interestingly, deprivation of the INS1 cells expressing PKD1-K612W from AA/serum or Glc/serum for 30 min resulted in a markedly decreased number of cells with the Golgi-localised PKD1-K612W (Supplementary fig. R11).

To assess activity of PKD1 in the TGN, I used a TGN-localized Fluorescence Resonance Energy Transfer (FRET) reporter (G-PKDrep-live) (Eisler, Fuchs et al. 2012) and performed time-lapse FRET measurements upon nutrient deprivation in INS1 cells. The FRET signal was rapidly and markedly decreased during deprivation of AA/serum or Glc/serum as compared to growing conditions, indicating inactivation of PKD1 in the TGN upon nutrient withdrawal (Fig. R4F).

9.4.3. Inactivation of PKD1 is necessary for SINGD

It was previously found in the laboratory that loss of the MAPK p38δ leads to enhanced PKD1 activity in β cells (Sumara, Formentini et al. 2009). To test if PKD1 controls SINGD, I performed QEM of β cells of fasted islets isolated from *p38δ* knockout ($p38\delta^{-/-}$) and control ($p38\delta^{+/+}$) mice. $p38\delta^{+/+}$ β cells displayed abundant lysosomes containing electron-dense SGs, which were markedly decreased in $p38\delta^{-/-}$ cells indicating reduced SINGD. In contrast, autophagic compartments were dramatically increased in starved $p38\delta^{-/-}$ β cells showing that

SINGD-dependent suppression of autophagy was diminished (Fig. R4G and quantification in Supplementary fig. R12). Our data thus suggest that PKD1 is a major regulator of SINGD in β cells.

9.5. Nutrient starvation response in β cells – a link to β cell function

The aforementioned findings strongly suggest that pancreatic β cells employ a very distinct cellular mechanism to overcome nutrient deprivation. In particular, starved β cells induce lysosomal degradation of nascent secretory insulin granules in the vicinity of the Golgi. Starvation-Induced Nascent Granule Degradation (SINGD) is controlled by Protein Kinase 1 (PKD1), a key player in Secretory Granule (SG) biogenesis. SINGD in turn triggers lysosomal recruitment and activation of mechanistic Target Of Rapamycin (mTOR) that suppresses autophagy.

Why do β cells employ such a distinct strategy to overcome nutrient deprivation? What is the physiological sense of this mechanism? The main systemic function of β cells is to control the whole body metabolism through secretion of insulin. Therefore, it is possible that response of β cells to nutrient deprivation is related to the regulation of metabolism. Under fasting conditions, when nutrient supply drops, insulin release is maintained at a low level. Unwanted insulin secretion from β cells during fasting results in a further decrease in Glc level in the blood, thus exacerbating fasting conditions (Gremlich, Nolan et al. 2005). Starvation-induced autophagy partially restores metabolic activity of the cell, by providing metabolites derived from degraded organelles and proteins. Since the metabolic activity in β cells is a major trigger of insulin secretion, induction of autophagy may thus lead to the increased secretion of insulin. Importantly, several metabolites generated through autophagy are known to promote insulin release (Prentki, Matschinsky et al. 2013). Since secreted insulin lowers blood Glc,

unwanted insulin secretion may in turn lead to a further increase of fasting-induced autophagy in starved β cell, resulting in further enhanced insulin secretion and thus providing a deleterious cycle leading to exhaustion of β cells and drop in blood Glc level. Based on these assumptions, it is possible to expect that observed suppression of autophagy in β cells during fasting contributes to fasting-induced suppression of insulin secretion. As shown in figure R3A, rapamycin treatment derepressed autophagy in starved INS1 cells. Therefore, to test the role of autophagy in fasting-induced suppression of insulin secretion, I treated INS1 cells with rapamycin at non-stimulatory Glc concentrations, corresponding to physiologic fasting Glc levels, and measured insulin release. Keeping autophagy high in β cells at non-stimulatory Glc levels precluded suppression of insulin secretion (Fig. R4H). This finding is in line with the previous report from our laboratory, in which it was shown that *p38δ*$^{-/-}$ mice, characterised by decreased SINGD and increased autophagy in their β cells, displayed higher fasting insulin release than control mice (Sumara, Formentini et al. 2009). In contrast, studies of mice, completely lacking autophagy in their β cells due to β-cell-specific ablation of the key autophagy gene ATG7, showed decreased fasting insulin level as compared to control mice (Ebato, Uchida et al. 2008; Jung, Chung et al. 2008). Therefore, suppression of autophagy in starved β cells may represent a strategy to avoid unwanted insulin secretion during fasting. SINGD, the alternative strategy to overcome nutrient deprivation, does also provide metabolites due to lysosomal degradation of SGs components. Why then activation of SINGD does not result in unwanted secretion of insulin? Interestingly, the newly formed SGs were shown to be preferentially released from β cells (Gold, Gishizky et al. 1982; Halban 1982; Michael, Xiong et al. 2007; Hou, Mogami et al. 2012). Therefore, targeting nascent SGs to lysosomes in SINGD provides nutrients that are needed to overcome fasting conditions and at the same time limits insulin secretion by depleting the "secretable" pool of SGs and by suppressing autophagy. Importantly, long-term fasting is expected to deplete β cells of

nascent SGs in the course of SINGD, which would in turn lead to the derepression of autophagy at some point, as no more "secretable" SGs would be targeted to the lysosomes. This explains upregulation of autophagy upon prolonged fasting for 24 and 48 hours, observed in primary β cells and β cell lines (Fujimoto, Hanson et al. 2009).

Altogether, rapid inactivation of PKD1 upon nutrient starvation results in SINGD, localized activation of mTOR and suppression of autophagy. On the other hand, PKD1 activity is required for proper SG biogenesis and subsequent insulin secretion. Thus, PKD1-dependent balance between SINGD and secretion contributes to maintenance of β cell function (Supplementary fig. R13).

9.6. A potential role of the SINGD-autophagy axis in Diabetes

Failure of pancreatic β cells is a hallmark of a relentless metabolic disorder – Diabetes mellitus, an increasingly prevailing disease which is currently affecting more than 350 million people worldwide (Danaei, Finucane et al. 2011; Whiting, Guariguata et al. 2011; Ashcroft and Rorsman 2012; Chen, Magliano et al. 2012). Therefore, identification of pathways, responsible for maintenance of β cell function is very important for understanding the mechanisms of this disease and for development of effective treatment strategies. Several studies revealed autophagy as a protective pathway against β cell failure. An increase in autophagy was found in β cells derived from diabetic patients and rodent models of Diabetes (Li, Zhang et al. 2006; Ebato, Uchida et al. 2008; Masini, Bugliani et al. 2009). In addition, upregulation of autophagy was shown to be protective against ER stress-induced Diabetes (Bachar-Wikstrom, Wikstrom et al. 2013). Furthermore, loss of autophagy results in compromised β cell function and leads to decreased β cell survival (Ebato, Uchida et al. 2008; Jung, Chung et al. 2008; Quan, Hur et al. 2012). It is important to note that $p38\delta^{-/-}$ mice,

which displayed decreased SINGD and increased autophagy (Fig. R4G), were found to be protected against β cell failure in a PKD1-dependent manner in a murine Diabetes model (Sumara, Formentini et al. 2009). Taking this into account, it would be very interesting to explore the potential role of the PKD1-dependent SINGD-autophagy axis in the context of Diabetes.

9.7. Outlook and perspectives

The mechanism of the fasting response identified in my study implies PKD1-dependent lysosomal degradation of nascent SGs, which in turn leads to suppression of autophagy via local activation of mTOR. These findings provoke several new questions, which will be very interesting to address in the future, such as identifying the molecular mechanisms of SINGD, exploring SINGD *in vivo*, unravelling the dynamics of PKD1-SINGD-autophagy pathway in the context of disease (diabetes) and investigating the specificity of this pathway in a cellular and evolutionary context.

9.7.1. Identification of molecular mechanisms of SINGD

In the nearest future, it will be important to identify molecular mechanisms downstream of PKD1, determining the destination of SGs either to secretory or to degradative pathways. As I have shown that kinase activity of PKD1 controls the fate of SGs, it is particularly important to identify the target(s) of PKD1 involved in these processes. Several strategies can be proposed to address this question:

1. An unbiased approach, based on the comparison of phosphoproteome of INS1 cells, stably expressing a wild type, constitutive active (S744E/S748E) and dominant negative PKD1 (K612W or K618N) will provide us a list of potential targets of PKD1 in pancreatic β cells. Phosphorylation by PKD1 is expected to protect SGs from SINGD. Therefore, for a secondary screen, I suggest to perform a genetic inactivation of identified hits (via knockdown or knockout), using stability of SGs as a readout, which can be easily assessed by measuring the levels of SGs markers, such as (Pro)insulin and Phogrin. As a next step, I will address the stability of SGs in INS1 cells expressing identified proteins, harbouring mutations

in the PKD1-dependent phosphorylation sites. For the confirmed hits I plan to explore their cellular localisation and phosphorylation by PKD1 under nutrient-rich and nutrient-poor conditions.

2. As a phosphoproteomic approach has certain limitations, for example, it is difficult to identify targets of PKD1 that are expressed at low levels, I will conduct another screen, similar to a secondary screen suggested above, including the libraries of genes, involved in the control of cellular traffic, secretion and degradation processes. Moreover, it would be very interesting to perform the same screen in PKD1 knockdown cells to find the genes responsible for targeting SGs to the lysosomes. A combination of these approaches will shed light on the molecular mechanisms of SINGD and on the origin of SINGD compartments.

3. Exploring the documented targets of PKD1 in pancreatic β cells may provide additional insights on the mechanisms of SINGD. For instance, BAR domain-containing protein Arfaptin 1 was recently identified in our laboratory as a target of PKD1 in pancreatic β cells. Phosphorylation of Arfaptin 1 by PKD1 is required for correct scission of SGs at the TGN (Gehart, Goginashvili et al. 2012). Expression of non-phosphorylatable mutant of Arfaptin 1 results in incomplete scission of SGs and therefore leads to accumulation of non-detached SGs in Golgi area. However, these SGs are not targeted to the lysosomes, thus indicating the involvement of other target(s) of PKD1 in SINGD. This being said, it will still be important to explore the alterations of Arfaptin1 phosphorylation upon nutrient deprivation and to address its potential cooperation with other target(s) of PKD1, involved in the control of SINGD.

A recently published phosphoproteomic study of INS1 cells has identified several potential targets of PKD1 (Han, Moon et al. 2012). Among them, transmembrane SG protein Phogrin, used as a SG marker in my studies, is of particular interest, as it was shown to function as phosphatidylinositol phosphatase, involved in the control of SGs trafficking and exocytosis

(Caromile, Oganesian et al. 2010). Intriguingly, deletion of Phogrin, as well as deletion of its close homologue IA-2 in mice results in a drastic decrease in number of SGs due to markedly increased lysosomal targeting and degradation of SGs (Cai, Hirai et al. 2011). Based on these observations, it is possible to assume that Phogrin is involved in the regulation of SINGD through PKD1. My preliminary data suggest that PKD1 phosphorylates the cytoplasmic tail of Phogrin at Ser 641, 681 and 687 *in vitro* (Supplementary fig. R14 – R16). Importantly, phosphorylation of Ser 687 in Phogrin was identified *in vivo* in the phosphoproteomic study mentioned above (Han, Moon et al. 2012). As a next step, I plan to explore the phosphorylation of Phogrin by PKD1 in INS1 cells comparing phosphorylation of Phogrin in INS1 cells, stably expressing a wild type, constitutive active and dominant negative PKD1. In addition, I aim at addressing PKD1-dependent phosphorylation of Phogrin under nutrient-rich and nutrient-poor conditions. If Phogrin is downstream of PKD1 in the regulation of SINGD, the disruption of PKD1-dependent phosphorylation of Phogrin will result in SINGD. Therefore, I plan to address the SGs dynamics in INS1 cells, expressing the unphosphorylatable mutants of Phogrin, using as a starting point S687A, S641A and S681A Phogrin mutants. If these experiments provide evidence for Phogrin to be a target of PKD1 in SINGD, the mechanisms of PKD1-dependent Phogrin activity will be explored, including the possible alterations of its phosphatidylinositol phosphatase activity in presence/absence of active PKD1, changes in its localisation and interactions with other proteins, involved in SGs trafficking.

The identification of target(s) of PKD1 in SINGD will provide us with the possibility to genetically dissect SINGD events and autophagy events and therefore to better understand the interaction between these pathways. Moreover, establishing the specific markers of SINGD will be very useful for biochemical characterisation of SINGD compartments.

9.7.2. PKD1-SINGD-autophagy pathway in healthy and disease state *in vivo*.

In my study, I characterised SINGD in the cellular models and in β cells of isolated primary islets. In the future, I plan to explore SINGD *in vivo*, for example, in fed and fasted mice. To do so, a combination of morphological and biochemical approaches can be suggested. First, I aim at visualiazing SINGD in β cells of fed and fasted mice with the help of immunohistochemistry, using markers of SGs, such as Pro(insulin) and lysosomes, such as Lamp1 or Lamp2. This approach will be corroborated with ultrastructural studies of these cells by electron microscopy, followed by immunogold labelling with SGs and lysosomal markers.

The findings shown in my study suggest the presence of a relatively high level of basal autophagy in non-fasted β cells. Taken together with the reported importance of basal autophagy in maintenance of β cells and in secretion of insulin (Ebato, Uchida et al. 2008; Jung, Chung et al. 2008), these observations suggest a functional significance of basal autophagy in β cells. One explanation for this phenomenon takes into account the well-established house-keeping role of autophagy, which relies on the clearance of damaged organelles and misfolded proteins: the highly specialized secretory machines, such as β cells, constantly face a danger of high ER stress and accumulation of misfolded proteins upon high secretory demand, and therefore autophagy might be used to protect the cells from the negative consequences of secretory burden (Bachar-Wikstrom, Wikstrom et al. 2013; Bachar-Wikstrom, Wikstrom et al. 2013). From another hand, aforementioned studies, together with my work, suggest a correlation between autophagy and secretion of insulin, thus raising an interesting possibility of a potential link between these pathways. Insulin secretion is driven by a high metabolic activity in β cells that relies on a high supply of nutrients. Do nutrients

derived from lysosomes participate in insulin secretion even in fed state? To address this question, it will be needed to study nutrient-induced insulin secretion while challenging autophagic and lysosomal activity, with the help of chemical compounds targeting cellular degradative pathways and by using genetic approaches (for example, by deleting lysosome-specific amino acid transporters).

Another important problem is the potential relevance of the PKD1-SINGD-autophagy pathway in the context of disease: Does the evolutionary adaptation of β cells to fasting play a role in failure of β cells in diabetes? To address this question, I plan to explore the identified mechanism in pre-diabetic/diabetic β cells. As a complementary approach, I would like to investigate a potential role of SINGD and/or suppression of autophagy in diabetes, by studying β cells from pre-diabetic/diabetic mice perturbing PKD1 activity. These changes will be induced acutely by PKD-specific inhibitors or genetically, with the help of $p38\delta^{-/-}$ and β cell-specific *PKD1* knockout mice or mice expressing constitutively active PKD1. As studies of autophagy-deficient and $p38\delta^{-/-}$ mice suggest a beneficial role of autophagy in diabetes, it would be interesting to develop tools, specifically triggering autophagy in β cells, for example, by chemical coupling of an autophagy-inducing drug, such as modified tat-beclin1 peptide (Shoji-Kawata, Sumpter et al. 2013), to the agonist of β cell-specific surface receptor.

9.7.3. Specificity of SINGD/autophagy in the cellular and evolutionary context.

Is the identified mechanism restricted to β cells? May it be relevant for other cell types, such as other secretory cells and/or cells involved in nutrient sensing? One good candidate cell type in which this should be tested is the pancreatic α cells, which secretes glucagon upon low Glc and insulin levels. It will be intriguing to test the levels of autophagy and SINGD in these

cells upon fasting and feeding conditions. Therefore, I plan to address levels of autophagy in α cells of fed and fasted LC3B-GFP expressing mice, with the approach shown in Fig. R1E, using glucagon as an α-cell marker. Furthermore, I will explore SINGD in these cells, using glucagon as SGs marker and Lamp1 or Lamp2 as a marker for lysosomes. Besides α cells, other classical cellular secretory models, which will be interesting to investigate in future in the context of the PKD1-SINGD-autophagy pathway, include Adrenocorticotropic Hormone (ACTH)-secreting Att-20 cells, catecholamines-secreting PC12 cells and Immunoglobulin-secreting plasma cells. With the help of genetic approaches, it will be a fascinating opportunity to expand these findings into a broader cellular and evolutionary context, by exploring PKD1-SINGD-autophagy pathway in a tissue-specific manner in simpler model organisms, like *C. elegans* or *D. melanogaster*. For example, it will be interesting to study these processes in secretory cells or neurons in these organisms. Addressing these questions will put the findings presented here in a broader context in cell biology and evolution.

9.8. Main figures

Figure R1. Nutrient depletion suppresses autophagy in β cells. (**A**) Immunofluorescence (IF) of LC3B-GFP puncta (white arrows) in INS1 cells under growing conditions (GC), without amino acids and fetal calf serum (no AA/FCS) or glucose (no Glc/FCS) for 2 and 6 hours. Quantification of LC3B-GFP puncta per cell (mean ± s. e. m.). $^{**}P<0.01$. (**B**) Live Fluorescence Microscopy of ptfLC3 puncta (white arrows) in INS1 cells. Pictures were captured at indicated time points after AA/FCS withdrawal. Merged, GFP and RFP signals are shown separately. (**C**) CLEM of ptfLC3 expressing INS1 cells under GC and no AA/FCS for 2 hours. EM, corresponding fluorescent and merged pictures are shown. Regions of interest (ROI) are indicated with labelled dashed squares. Yellow and black arrows indicate autophagosomes and autolysosomes, respectively. (**D**) Western blot of LC3B using lysates of INS1 cells treated with BafA1, 10 nM under GC and no AA/FCS for indicated time points. GAPDH was used as a loading control. (**E**) IF of LC3B-GFP puncta (white arrows) and insulin (red) in β cells in islets of fed and fasted LC3B-GFP expressing mice. The nucleus was stained with DAPI. Quantification of LC3B-GFP puncta per 1600 μm^2(mean ± s. e. m.). $^{**}P<0.01$.

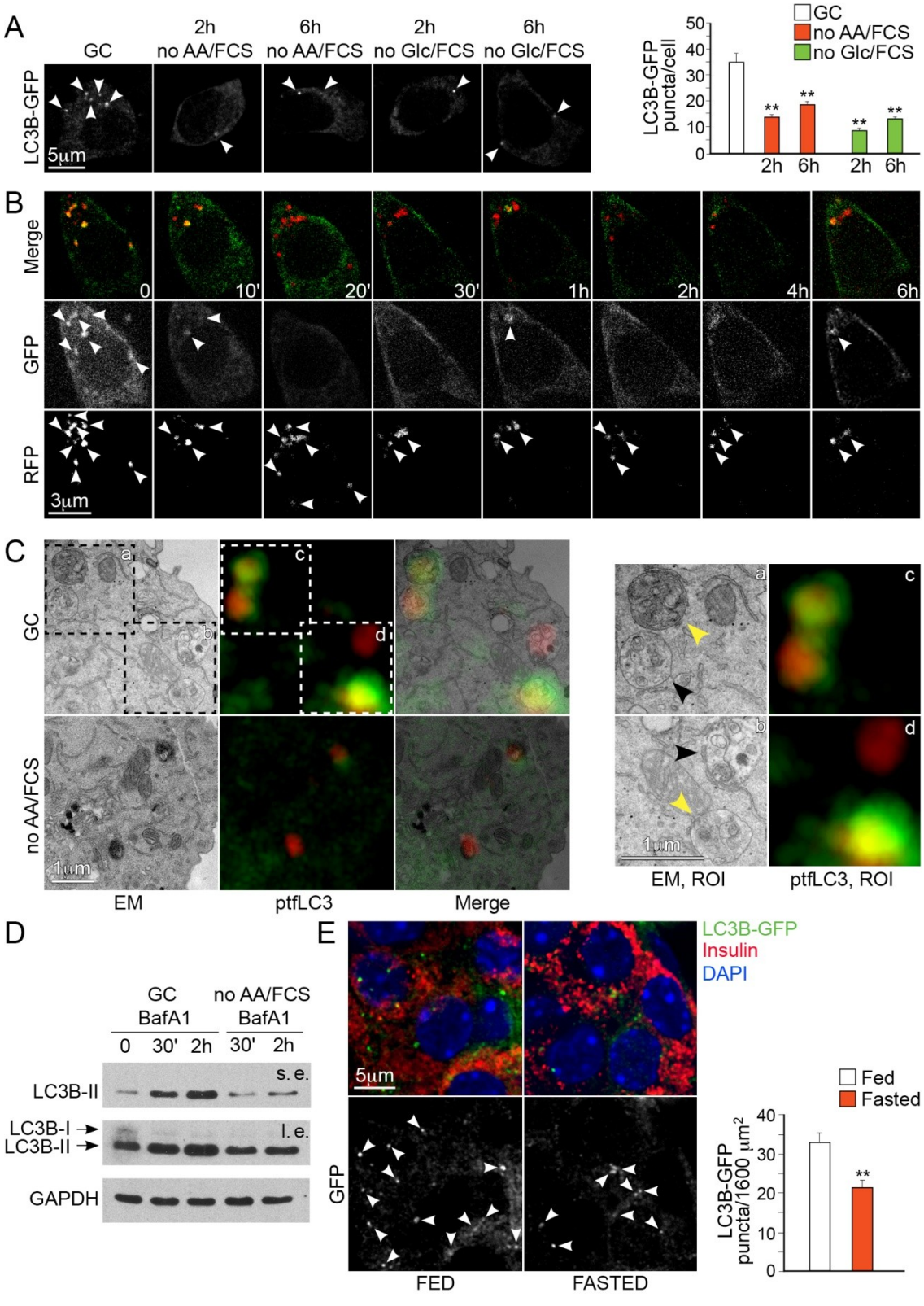
A
GC
2h no AA/FCS
6h no AA/FCS
2h no Glc/FCS
6h no Glc/FCS
LC3B-GFP
5μm
LC3B-GFP puncta/cell
GC
no AA/FCS
no Glc/FCS
B
Merge
GFP
RFP
0
10'
20'
30'
1h
2h
4h
6h
3μm
C
GC
no AA/FCS
EM
ptfLC3
Merge
EM, ROI
ptfLC3, ROI
D
GC BafA1
no AA/FCS BafA1
0 30' 2h 30' 2h
LC3B-II
s.e.
LC3B-I
LC3B-II
l.e.
GAPDH
E
LC3B-GFP
Insulin
DAPI
5μm
GFP
FED
FASTED
Fed
Fasted
LC3B-GFP puncta/1600 μm²

Figure R1

Figure R2. Nutrient depletion induces SINGD in β cells. (**A**) Immunofluorescence (IF) of Phogrin and Lamp1 in INS1 cells under growing conditions (GC) or without amino acids and fetal calf serum (no AA/FCS) for 2 hours. Regions of interest (ROI) are indicated with dashed squares. White arrows indicate co-localization of Phogrin with Lamp1. A Golgi marker (pGolgi-CFP) was used. Quantification of co-localization of Phogrin and Lamp1 per cell (mean ± s. e. m.). $^{**}P<0.01$. (**B**) CLEM of INS1 cells co-expressing Phogrin-GFP and Lamp1-RFP under GC and no AA/FCS for 2 hours. EM, corresponding fluorescent and merged pictures are shown. Regions of interest (ROI) are indicated with dashed squares. White arrows indicate co-localization of Phogrin-GFP with Lamp1-RFP. Yellow arrows indicate lysosomes correlated to co-localized Phogrin-GFP and Lamp1-RFP. (**C**) IF of Phogrin and Lamp1 in INS1 cells treated with lysosomal inhibitors under GC and no AA/FCS for 2 hours. A Golgi marker (pGolgi-CFP) was used. (**D**) Western blot of proinsulin using lysates of INS1 cells treated or not with lysosomal inhibitors (LI) under GC and no AA/FCS for 6 hours. GAPDH was used as a loading control. (**E**) EM of Golgi areas in primary murine islets under GC and no AA/FCS for 2 hours. Yellow arrows indicate secretory granules-containing lysosomes. Quantification in **Supplementary fig. R6**.

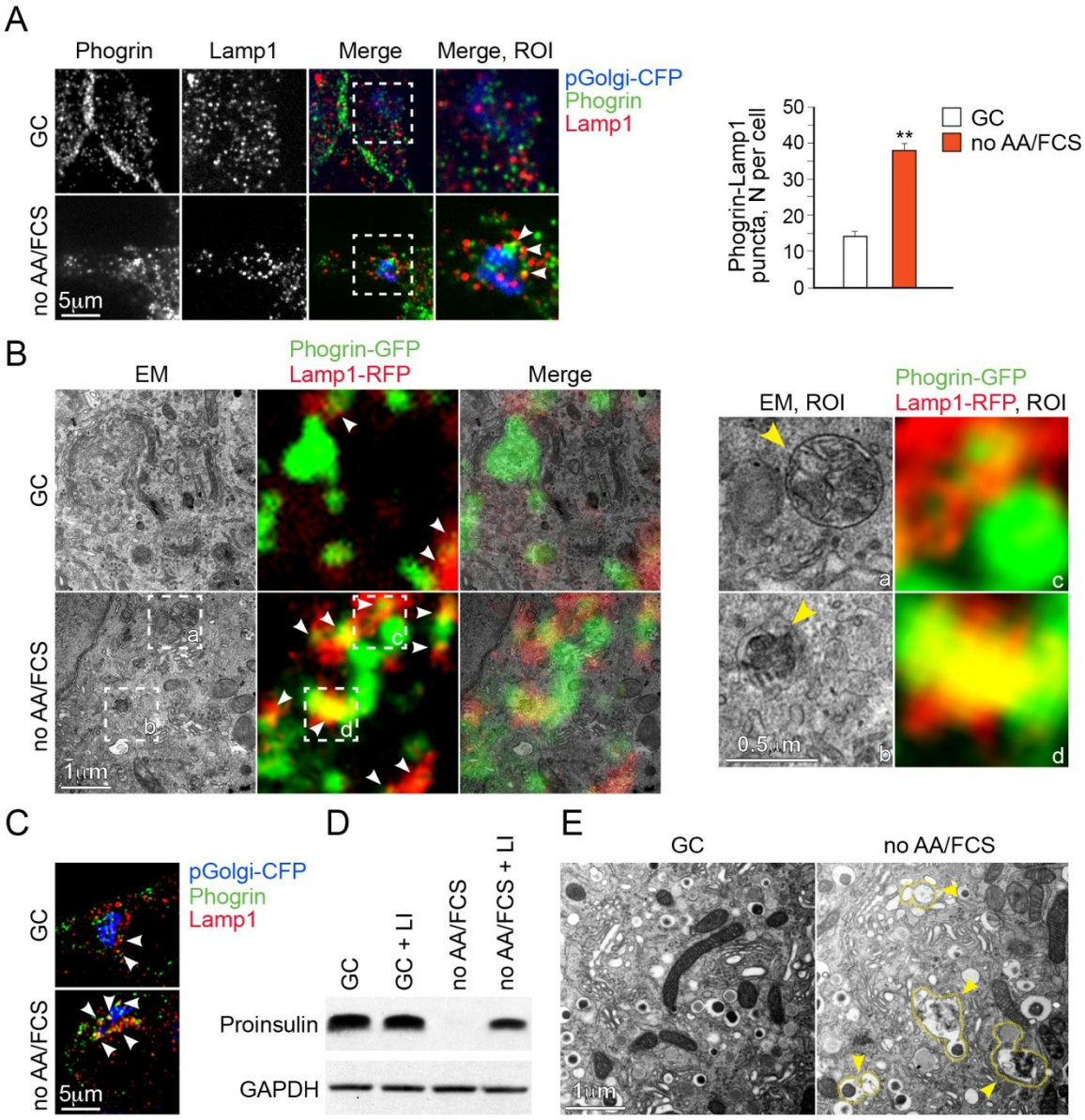
A
Phogrin
Lamp1
Merge
Merge, ROI
GC
no AA/FCS
5μm
pGolgi-CFP
Phogrin
Lamp1
Phogrin-Lamp1 puncta, N per cell
50
40
30
20
10
0
**
GC
no AA/FCS
B
EM
Phogrin-GFP
Lamp1-RFP
Merge
GC
no AA/FCS
a
b
c
d
1μm
EM, ROI
Phogrin-GFP
Lamp1-RFP, ROI
0.5μm
C
pGolgi-CFP
Phogrin
Lamp1
GC
no AA/FCS
5μm
D
GC
GC + LI
no AA/FCS
no AA/FCS + LI
Proinsulin
GAPDH
E
GC
no AA/FCS
1μm

Figure R2

Figure R3. SINGD suppresses autophagy in an mTOR-dependent manner. (**A**) IF of LC3B-GFP puncta (white arrows) in INS1 cells under growing conditions (GC) or without amino acids and fetal calf serum (no AA/FCS) for 2 hours treated or not with rapamycin, 100 nM or torin-1, 250 nM as indicated. Quantification of LC3B-GFP puncta per cell (mean ± s. e. m.). $^{**}P<0.01$. (**B**) Immunofluorescence (IF) of mTOR in INS1 cells co-expressing Phogrin-GFP and Lamp1-RFP under GC and no AA/FCS for 2 hours. White arrows in regions of interest (ROI) highlighted with dashed squares indicate co-localization of Phogrin-GFP with mTOR and Phogrin-GFP with Lamp1-RFP. A Golgi marker (Giantin) was used. (**C**) Western blot of indicated proteins using lysates of INS1 cells treated or not with rapamycin, 100 nM under GC, no AA/FCS or without glucose/fetal calf serum (no Glc/FCS) for 2 hours. GAPDH was used as a loading control. (**D**) IF of phosphorylated ULK1 (S757-ULK1) in INS1 cells co-expressing Phogrin-GFP and Lamp1-RFP under GC and no AA/FCS for 2 hours. ROI are indicated with dashed squares. White arrows in ROI indicate co-localization of Phogrin-GFP with Lamp1-RFP and S757-ULK1. A Golgi marker (Giantin) was used.

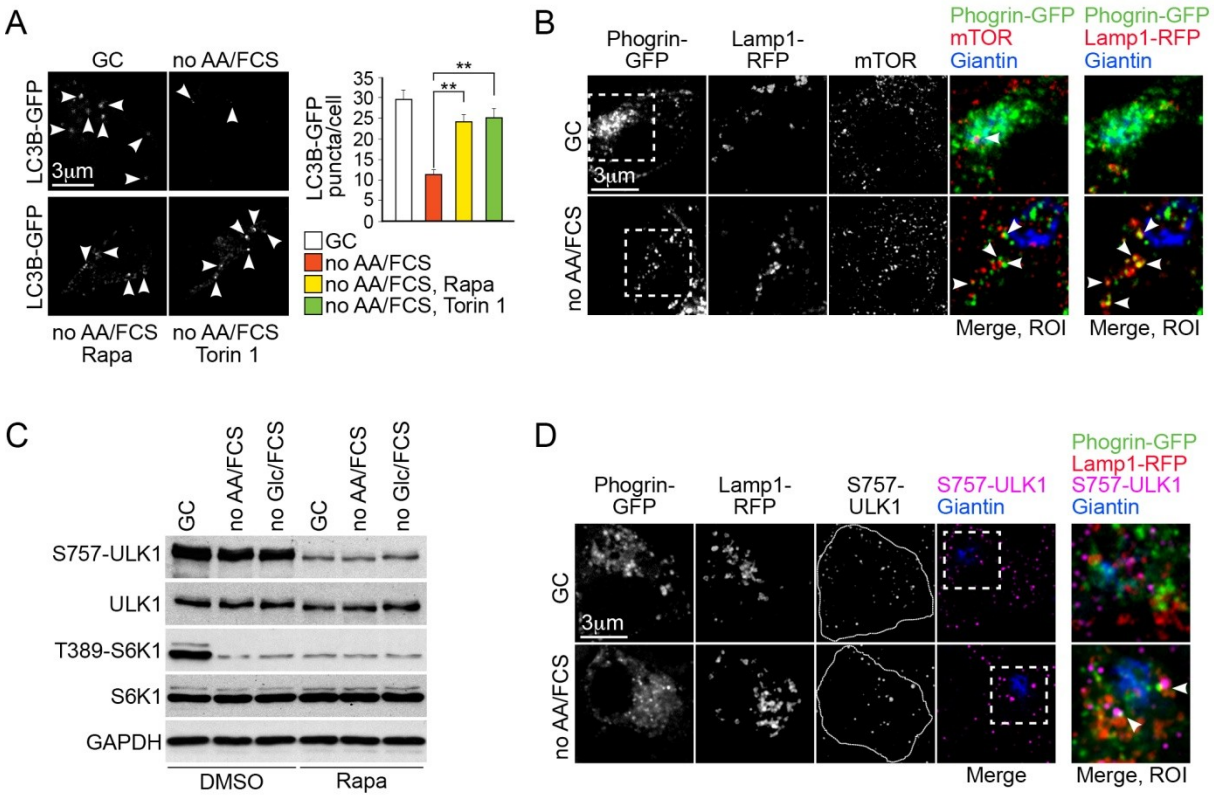
A
GC
no AA/FCS
LC3B-GFP
3μm
LC3B-GFP
no AA/FCS Rapa
no AA/FCS Torin 1
LC3B-GFP puncta/cell
35
30
25
20
15
10
5
0
**
**
GC
no AA/FCS
no AA/FCS, Rapa
no AA/FCS, Torin 1
B
Phogrin-GFP
Lamp1-RFP
mTOR
Phogrin-GFP mTOR Giantin
Phogrin-GFP Lamp1-RFP Giantin
GC
3μm
no AA/FCS
Merge, ROI
Merge, ROI
C
GC
no AA/FCS
no Glc/FCS
GC
no AA/FCS
no Glc/FCS
S757-ULK1
ULK1
T389-S6K1
S6K1
GAPDH
DMSO
Rapa
D
Phogrin-GFP
Lamp1-RFP
S757-ULK1
S757-ULK1 Giantin
Phogrin-GFP Lamp1-RFP S757-ULK1 Giantin
GC
3μm
no AA/FCS
Merge
Merge, ROI

Figure R3

Figure R4. PKD1 is both necessary and sufficient in SINGD. (**A**) Western blot of proinsulin using lysates of INS1 cells treated with CID755673 for indicated times. GAPDH was used as a loading control. (**B**) EM of Golgi areas in non-silenced and PKD1-depleted (shPKD1) INS1 cells. Yellow arrows indicate secretory granules-containing lysosomes (GCLs). Quantification in Supplementary fig. R9. (**C**) Immunofluorescence (IF) of mTOR and Lamp2 in non-silenced and PKD1-depleted (shPKD1) INS1 cells. White arrows indicate co-localization of mTOR with Lamp2. The nucleus was stained with DAPI. (**D**) Western blot of indicated proteins using lysates of non-silenced and PKD1-depleted (shPKD1) INS1 cells. GAPDH was used as a loading control. (**E**) Western blot of LC3B using lysates of non-silenced and PKD1-depleted (shPKD1) INS1 cells treated with BafA1 at indicated concentrations for indicated times. GAPDH was used as a loading control. (**F**) Live-cell FRET assay in INS1 cells expressing G-PKDrep-live under growing culture (GC) conditions, without amino acids and fetal calf serum (no AA/FCS) or without glucose/FCS (no Glc/FCS). FRET was measured and expressed as normalized YFP-C/CFP ratios during a time course as indicated. (**G**) Upper panel: EM of Golgi areas of fasted β cells in primary islets of $p38\delta^{+/+}$ and $p38\delta^{-/-}$ mice. Yellow arrows indicate secretory GCLs. Lower panel : EM of cytoplasm of fasted β cells in primary islets of $p38\delta^{+/+}$ and $p38\delta^{-/-}$ mice. The yellow arrow indicates an autophagosome. Quantifications in Supplementary fig. R10. (**H**) Insulin in supernatants of INS1 cells treated with non-stimulatory 2.8 mM Glc in presence of DMSO or rapamycin. Insulin concentrations are expressed as a percentage of DMSO control (mean ± s. e. m.).

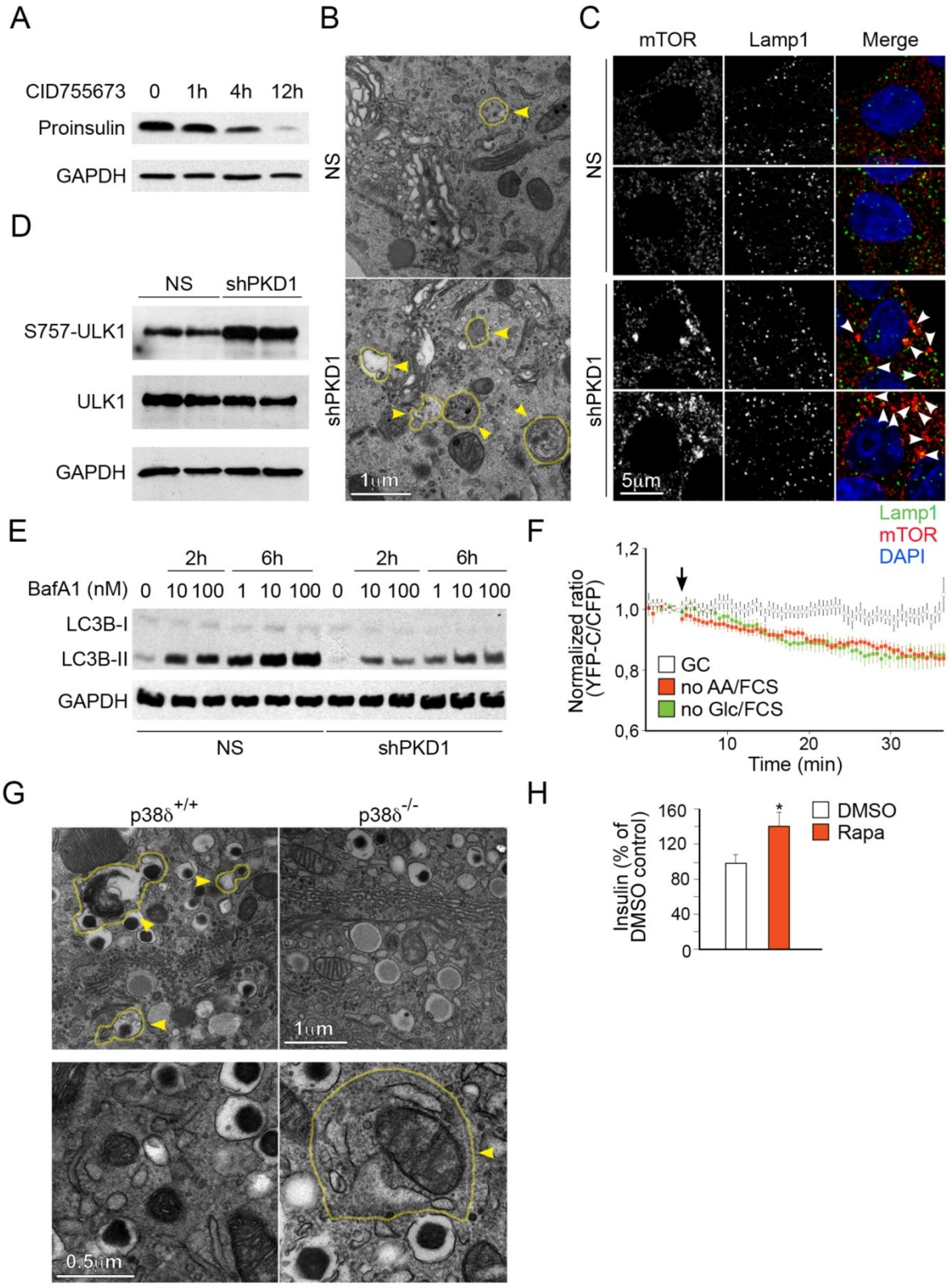
A
CID755673 0 1h 4h 12h
Proinsulin
GAPDH
B
NS
shPKD1
1µm
C
mTOR
Lamp1
Merge
NS
shPKD1
5µm
D
NS shPKD1
S757-ULK1
ULK1
GAPDH
E
2h 6h 2h 6h
BafA1 (nM) 0 10 100 1 10 100 0 10 100 1 10 100
LC3B-I
LC3B-II
GAPDH
NS
shPKD1
F
Lamp1
mTOR
DAPI
Normalized ratio (YFP-C/CFP)
1,2
1,0
0,8
0,6
GC
no AA/FCS
no Glc/FCS
10
20
30
Time (min)
G
p38δ+/+
p38δ-/-
1µm
0.5µm
H
Insulin (% of DMSO control)
160
120
80
40
0
*
DMSO
Rapa

Figure R4

9.9. Supplementary figures

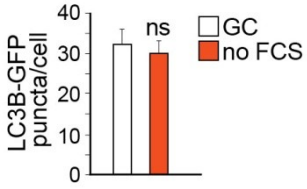

Supplementary Figure R1. Deprivation from serum alone did not affect LC3B-GFP puncta in starved INS1 cells. Quantification of LC3B-GFP puncta per cell in INS1 cells under growing conditions (GC) and without fetal calf serum (FCS) (mean ± s.e.m.). ns: not significant.

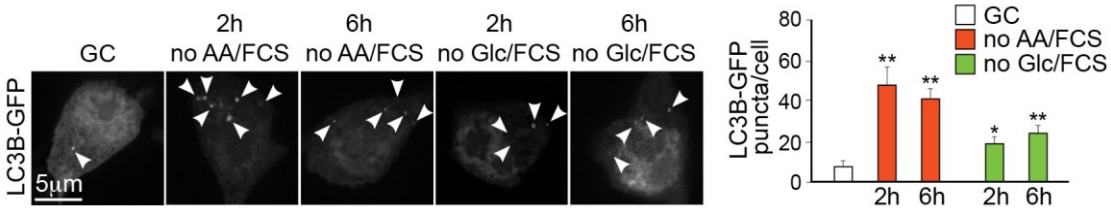

Supplementary Figure R2. LC3B-GFP puncta increase in HEK293T cells upon nutrient starvation. Immunofluorescence (IF) of LC3B-GFP puncta (white arrows) in HEK293T cells under growing conditions (GC), without amino acids and fetal calf serum (no AA/FCS) or glucose/FCS (no Glc/FCS) for 2 and 6 hours. Quantification of LC3B-GFP puncta per cell (mean ± s.e.m.). *P<0.05,**P<0.01.

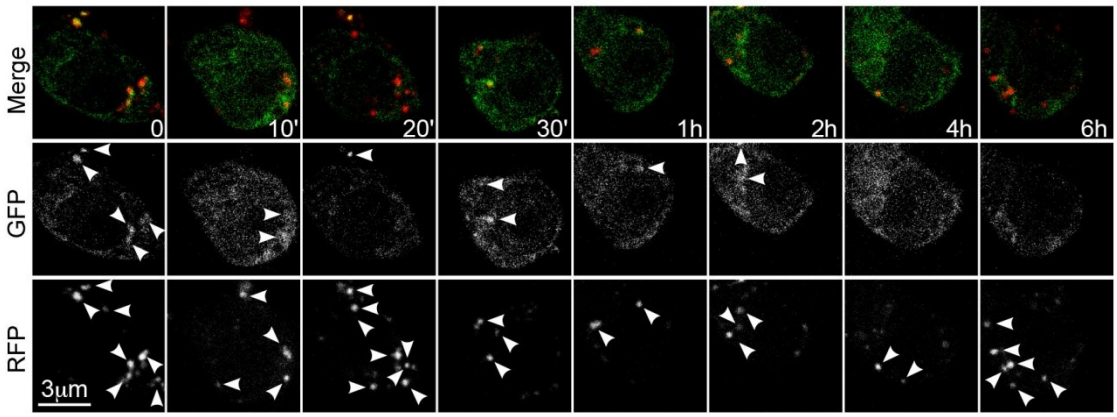

Supplementary Figure R3. Reduced autophagic flux in INS1 cells upon glucose (Glc) and fetal calf serum (FCS) withdrawal. Live Fluorescence Microscopy of ptfLC3 puncta (white arrows) in INS1 cells. Pictures were captured at indicated time points after Glc/FCS withdrawal. Merged, GFP and RFP signals are shown separately.

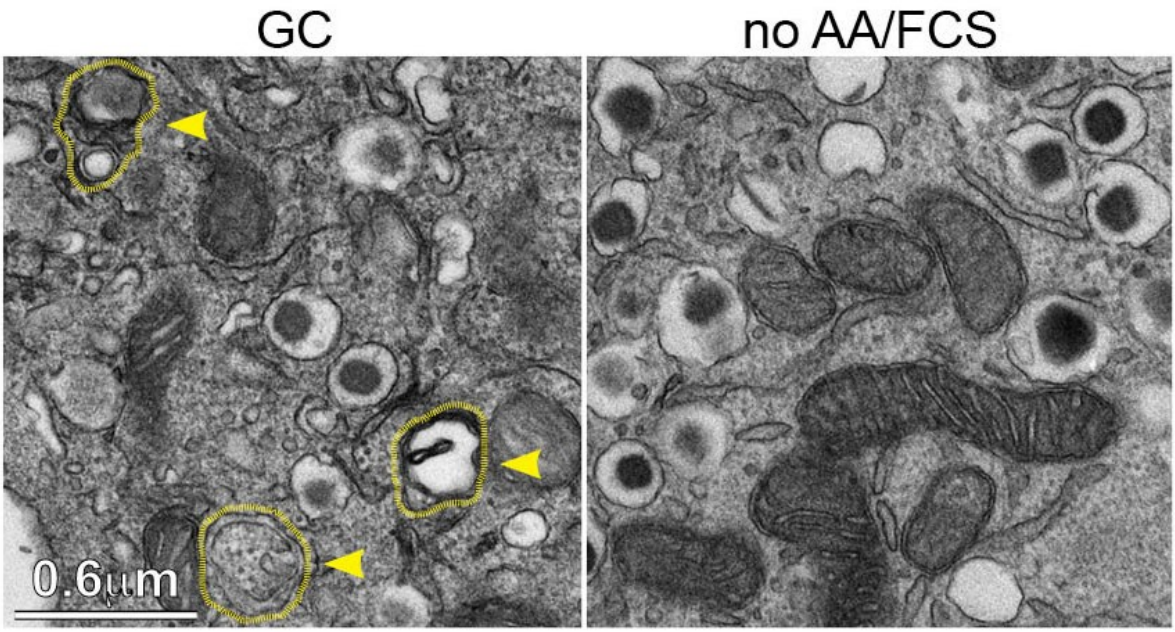

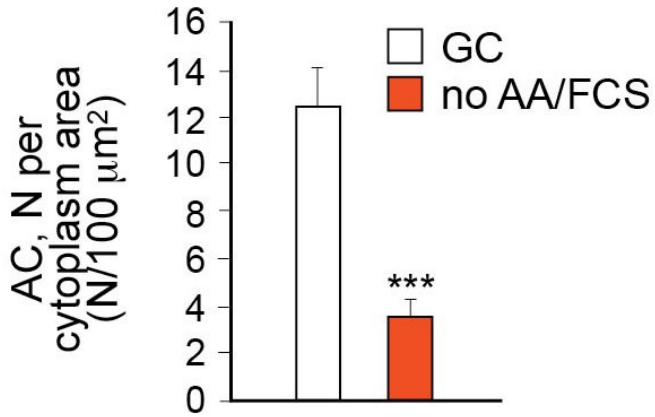

Supplementary Figure R4. Autophagic compartments (AC) decrease in β cells in primary murine islets upon AA/serum deprivation. Electron microscopy of cytoplasm areas in β cells in primary murine islets under growing culture (GC) conditions or without AA and fetal calf serum (no AA/FCS) for 2 hours. Yellow arrows indicate ACs. Quantification of ACs per 100 μm2 (mean ± s.e.m.). ***P<0.001.

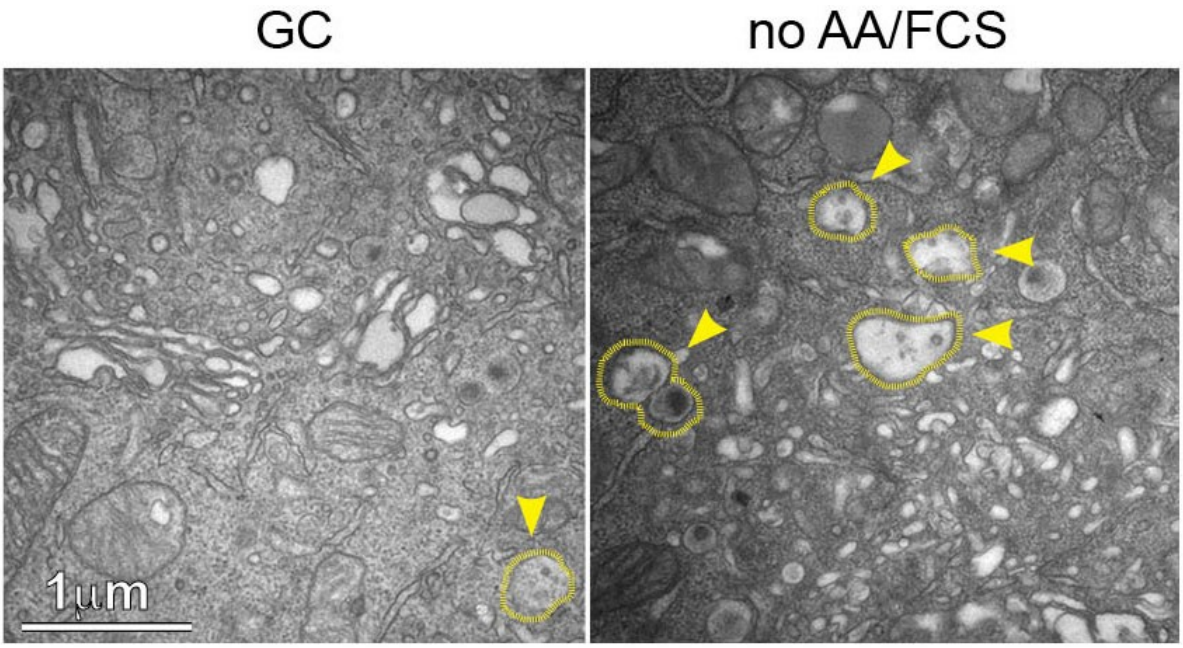

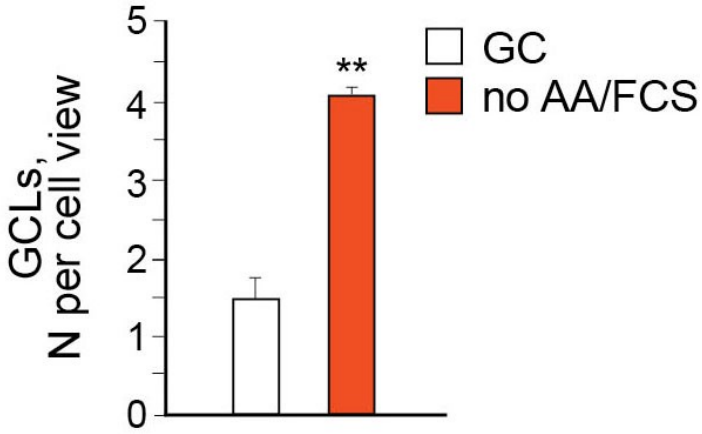

Supplementary Figure R5. Granule containing lysosomes (GCLs) increase in INS1 cells upon AA/serum deprivation. Electron microscopy of Golgi areas in INS1 cells under growing culture (GC) conditions or without AA and fetal calf serum (no AA/FCS) for 2 hours. Yellow arrows indicate GCLs. Quantification of GCLs (mean ± s.e.m.). **P<0.01.

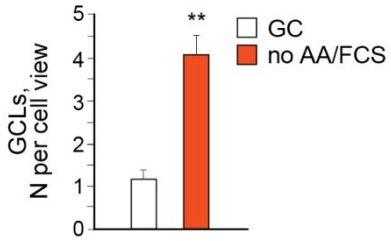

Supplementary Figure R6. Granule containing lysosomes (GCLs) increase in β cells in primary murine islets upon AA/serum deprivation. Quantification of GCLs in Golgi areas of β cells in primary murine islets under growing culture (GC) conditions or without AA and fetal calf serum (no AA/FCS) for 2 hours (mean ± s.e.m.). **P<0.01.

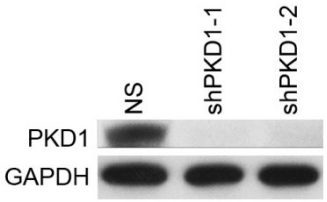

Supplementary Figure R7. Short hairpin-mediated knockdown of PKD1 in INS1 cells. Western blot of PKD1 using lysates of INS1 cells stably expressing two different short hairpin RNAs against PKD1 (shPKD1-1 and shPKD1-2) or non-silencing shRNA. shPKD1-1 is shown in further experiments. GAPDH is used as a loading control.

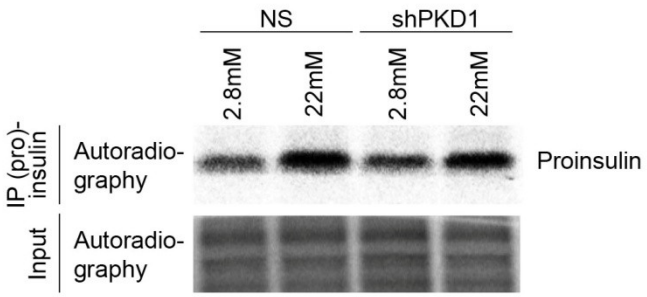

Supplementary Figure R8. PKD1 knockdown in INS1 cells does not alter proinsulin biosynthesis. Autoradiography of immunoprecipitated proinsulin using lysates of INS1 cells transfected with short hairpin RNA against PKD1 (shRNA) compared to cells transfected with non-silencing shRNA (NS) and incubated with indicated concentrations of glucose in presence of [35S]-methionine. Autoradiography of total input was used as a loading control.

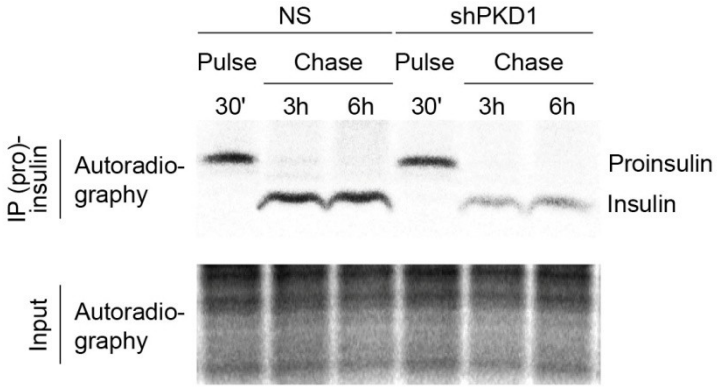

Supplementary Figure R9. PKD1 knockdown in INS1 cells decreases accumulation of newly formed insulin. Autoradiography of immunoprecipitated proinsulin/insulin using lysates of INS1 cells transfected with short hairpin RNA against PKD1 (shRNA) compared to cells transfected with non-silencing shRNA (NS) and incubated for 30 minutes with [35S]-methionine (pulse) followed by chase for indicated times. Autoradiography of total input was used as a loading control.

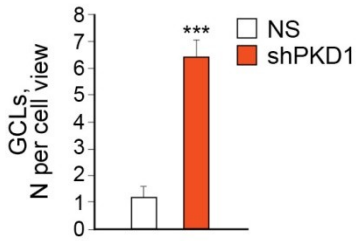

Supplementary Figure R10. Increased granule containing lysosomes (GCLs) in INS1 cells depleted of PKD1. Quantification of GCLs in INS1 cells transfected with short hairpin RNA against PKD1 (shRNA) compared to cells transfected with non-silencing shRNA (NS) (mean ± s.e.m.). ***P<0.001. Representative EM pictures are shown in Figure R4B.

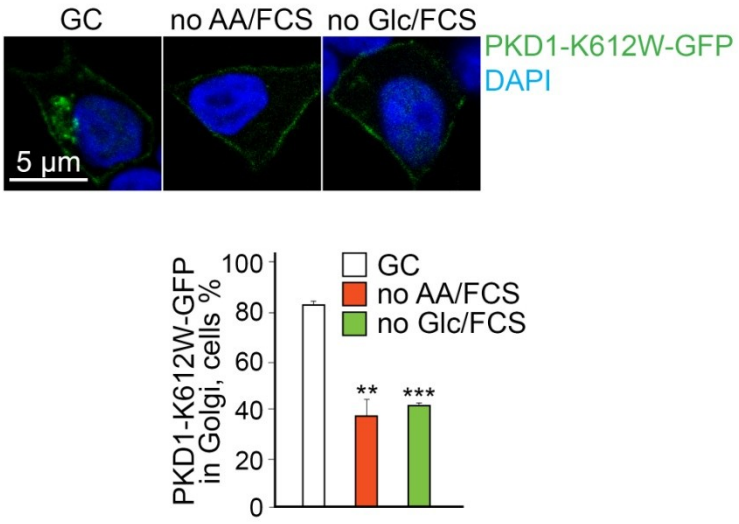

Supplementary Figure R11. Nutrient deprivation decreases Golgi-specific localisation of PKD1-K612W-GFP in INS1 cells. Immunofluorescence (IF) of PKD1-K612W-GFP in INS1 cells under growing conditions (GC), without amino acids and fetal calf serum (no AA/FCS) or glucose/FCS (no Glc/FCS) for 30 minutes. The nucleus was stained with DAPI. Percentage of INS1 cells with PKD1-K612W-GFP in Golgi (mean ± s.e.m.). **P<0.01, ***P<0.001.

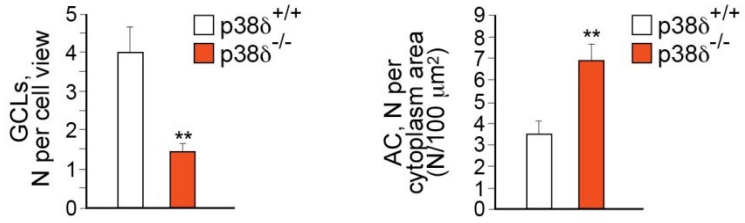

Supplementary Figure R12. Granule containing lysosomes (GCLs) decrease and autophagic compartments (AC) increase in β cells in fasted primary murine islets of p38δ-/- mice Quantification of GCLs in Golgi areas and of ACs in cytoplasm areas per 100 μm2 of β cells in islets of mice as indicated (mean ± s.e.m.). **P<0.01. Representative EM pictures are shown in Figure R4G.

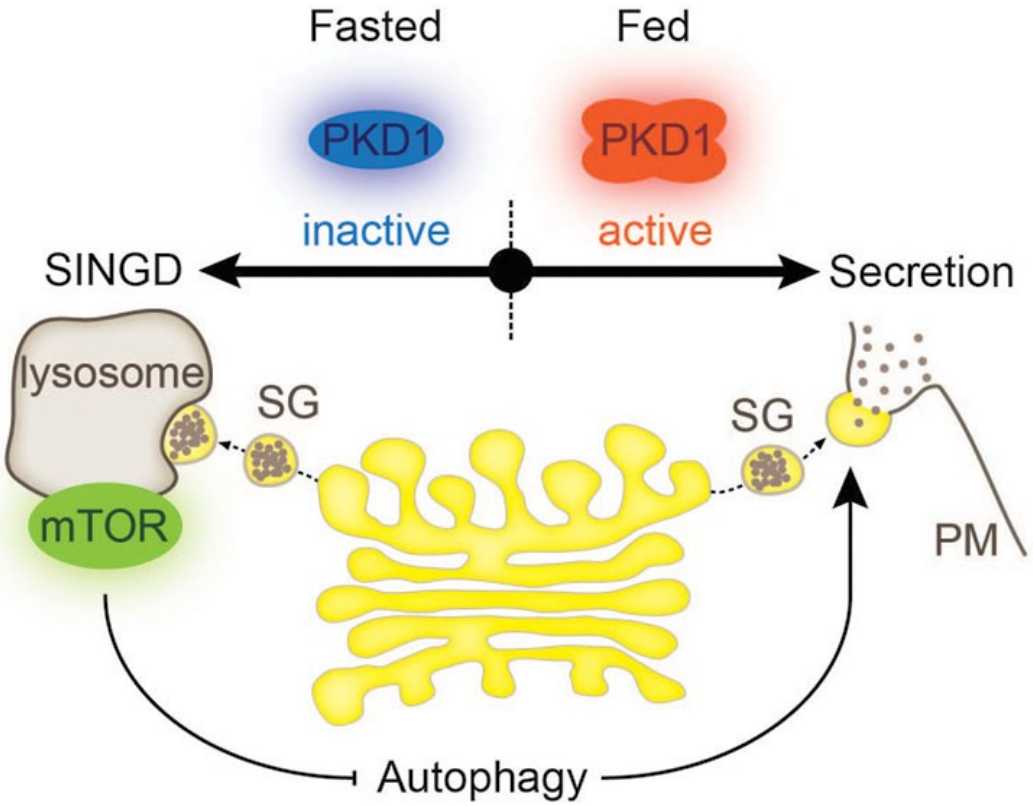

Supplementary Figure R13. Model highlighting links between SINGD, secretion and autophagy SG : secretory granule, PM : plasma membrane.

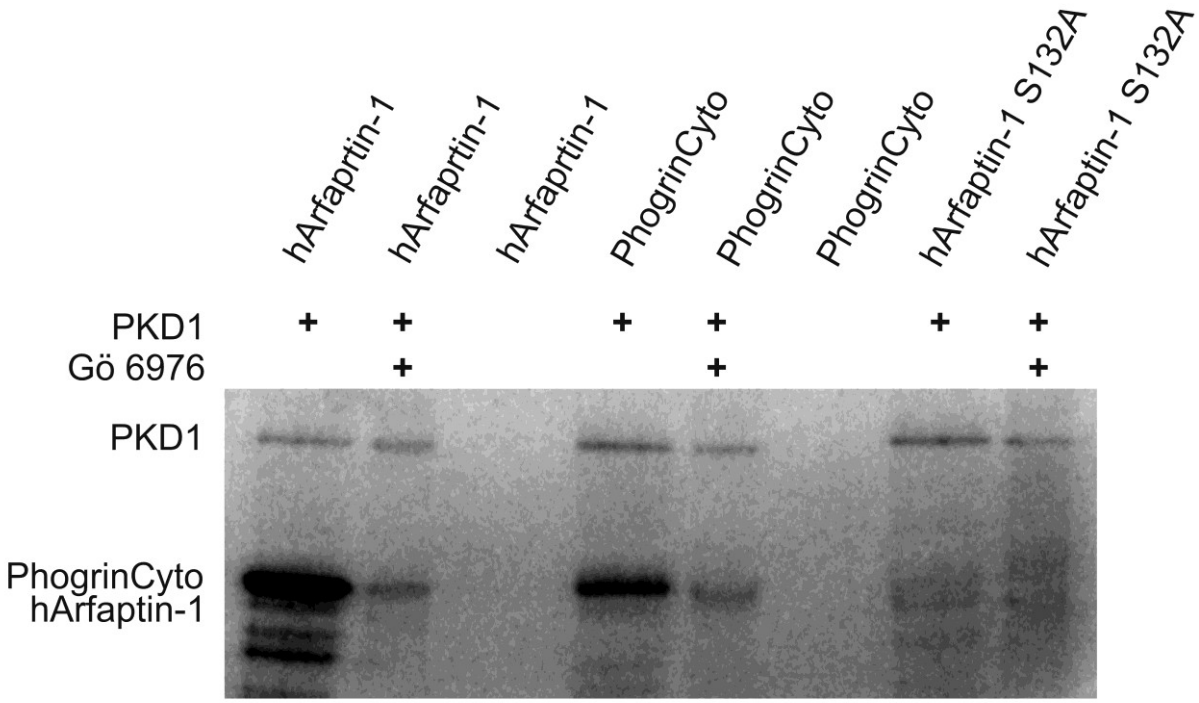

Supplementary Figure R14. PKD1 phosphorylates cytoplasmic tail of Phogrin (PhogrinCyto) *in vitro*. Autoradiography of in vitro kinase assay using recombinant GST-tagged cytoplasmic tail of Phogrin PhogrinCyto (69 kDa) after addition of recombinant PKD1 without or with the PKD inhibitor Gö 6976. Wild-type human Arfaptin-1 (hArfaptin-1, 68 kDa) and serine to alanine mutant Arfaptin-1 (hArfaptin-1 S132A) were used as positive and negative controls respectively.

Supplementary Figure R15. Phosphorylation of PhogrinCyto by PKD1 in vitro revealed by mass-spectrometry. Sequence coverage: 92.11 %. 3 phosphorylation sites were identified: S17, S57 and S63, corresponding to S641, S681 and S687 in full-length Phogrin respectively.

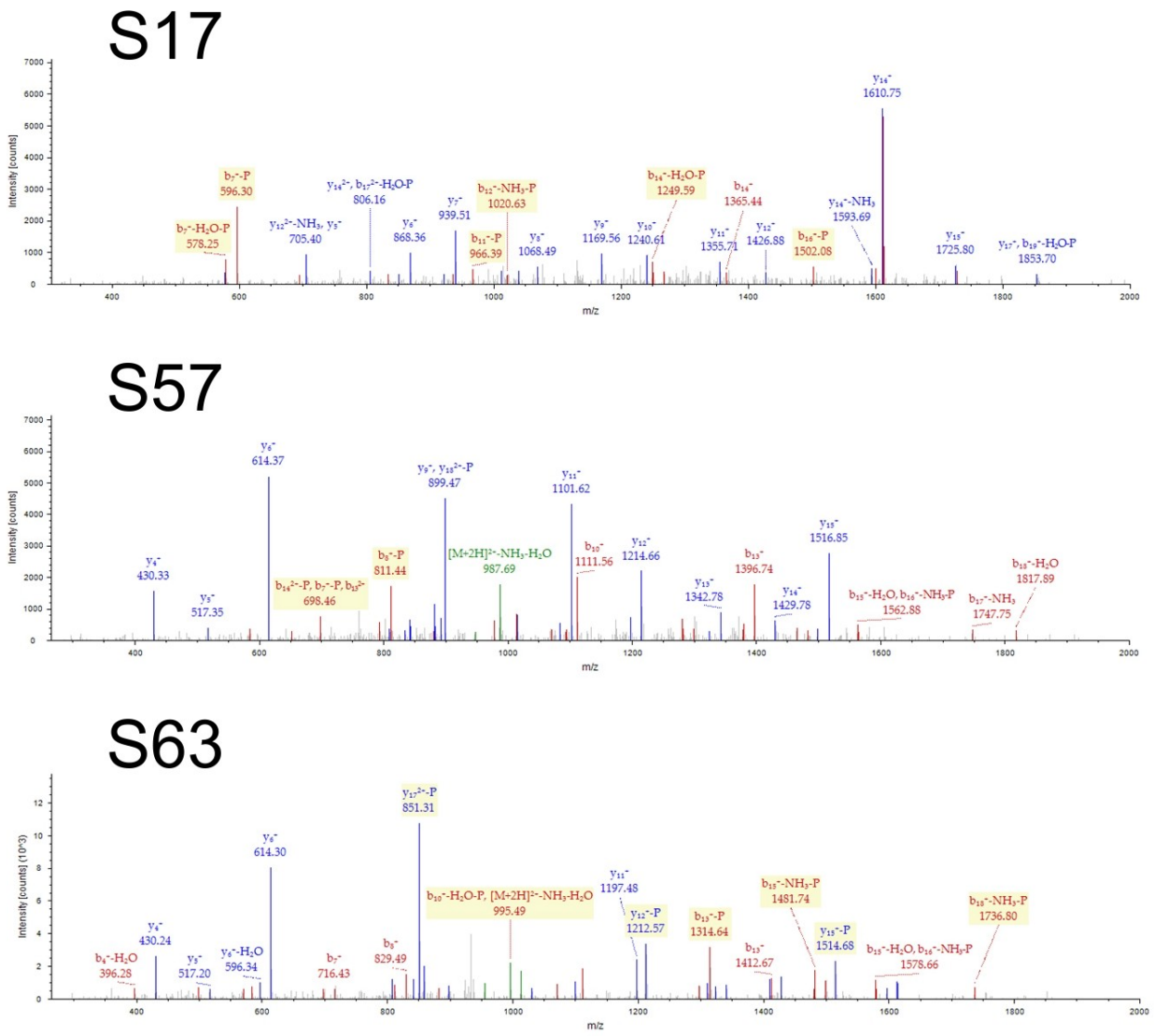

Supplementary Figure R16. Spectrum details of phosphorylation sites of PhogrinCyto.

10. Acknowledgements

I will always remember my time here in IGBMC, where almost every scientific endeavour can be approached. I greatly appreciate my advisor Romeo Ricci for providing me invaluable freedom and support, for both his patience and impatience, and for his encouraging inputs and insights that followed me all the days in his lab. I am forever indebted to all the members of Ricci lab for creating a genuinely friendly and supportive atmosphere, where a sin of boredom can never be experienced. Our joined seminars of Sumara and Ricci groups were always giving me a broader prospective of my work and a motivation to go further. I would like to thank Iza and all the members of her group for providing these inputs and for being extremely friendly and helpful.

I am very happy to acknowledge Ernst Hafen and Robbie Loewith for participating in my Thesis Committee, for taking their time and for the scientific discussions that greatly helped me with accomplishing my studies.

My research aims were not be achievable without a highly collaborative nature of IGBMC. I am particularly thankful to Yannick Schwab for guiding me into the fascinating world of Electron Microscopy and to Pascal Kessler, Marc Koch and Coralie Spiegelhalter for their generous help with the cutting edge imaging.

I would like to thank Oleg Tikhodeyev and Ludmila Mironova, whose guidance and mentorship had brought me into the field of biological research. I am absolutely grateful to my family for the continuous support and encouragement, for the warmth I feel every day. I have an extreme and exceptional luck to share my family and scientific life with Ksenia, who made all this to be possible.

11. References

Ashcroft, F. M. and P. Rorsman (2012). "Diabetes mellitus and the beta cell: the last ten years." Cell **148**(6): 1160-1171.

Bachar-Wikstrom, E., J. D. Wikstrom, et al. (2013). "Stimulation of autophagy improves endoplasmic reticulum stress-induced diabetes." Diabetes **62**(4): 1227-1237.

Bachar-Wikstrom, E., J. D. Wikstrom, et al. (2013). "Improvement of ER stress-induced diabetes by stimulating autophagy." Autophagy **9**(4): 626-628.

Bar-Peled, L., L. Chantranupong, et al. (2013). "A Tumor suppressor complex with GAP activity for the Rag GTPases that signal amino acid sufficiency to mTORC1." Science **340**(6136): 1100-1106.

Bar-Peled, L., L. D. Schweitzer, et al. (2012). "Ragulator is a GEF for the rag GTPases that signal amino acid levels to mTORC1." Cell **150**(6): 1196-1208.

Baron, C. L. and V. Malhotra (2002). "Role of diacylglycerol in PKD recruitment to the TGN and protein transport to the plasma membrane." Science **295**(5553): 325-328.

Ben-Sahra, I., J. J. Howell, et al. (2013). "Stimulation of de novo pyrimidine synthesis by growth signaling through mTOR and S6K1." Science **339**(6125): 1323-1328.

Betz, C. and M. N. Hall (2013). "Where is mTOR and what is it doing there?" The Journal of cell biology **203**(4): 563-574.

Binda, M., M. P. Peli-Gulli, et al. (2009). "The Vam6 GEF controls TORC1 by activating the EGO complex." Molecular cell **35**(5): 563-573.

Blommaart, E. F., J. J. Luiken, et al. (1995). "Phosphorylation of ribosomal protein S6 is inhibitory for autophagy in isolated rat hepatocytes." The Journal of biological chemistry **270**(5): 2320-2326.

Cai, T., H. Hirai, et al. (2011). "Deletion of Ia-2 and/or Ia-2beta in mice decreases insulin secretion by reducing the number of dense core vesicles." Diabetologia **54**(9): 2347-2357.

Caromile, L. A., A. Oganesian, et al. (2010). "The neurosecretory vesicle protein phogrin functions as a phosphatidylinositol phosphatase to regulate insulin secretion." The Journal of biological chemistry **285**(14): 10487-10496.

Chan, E. Y., S. Kir, et al. (2007). "siRNA screening of the kinome identifies ULK1 as a multidomain modulator of autophagy." The Journal of biological chemistry **282**(35): 25464-25474.

Chauvin, C., V. Koka, et al. (2014). "Ribosomal protein S6 kinase activity controls the ribosome biogenesis transcriptional program." Oncogene **33**(4): 474-483.

Chen, L., D. J. Magliano, et al. (2012). "The worldwide epidemiology of type 2 diabetes mellitus--present and future perspectives." Nature reviews. Endocrinology **8**(4): 228-236.

Cheong, H., T. Lindsten, et al. (2011). "Ammonia-induced autophagy is independent of ULK1/ULK2 kinases." Proceedings of the National Academy of Sciences of the United States of America **108**(27): 11121-11126.

Clark, S. L., Jr. (1957). "Cellular differentiation in the kidneys of newborn mice studies with the electron microscope." The Journal of biophysical and biochemical cytology **3**(3): 349-362.

Cruz-Garcia, D., M. Ortega-Bellido, et al. (2013). "Recruitment of arfaptins to the trans-Golgi network by PI(4)P and their involvement in cargo export." The EMBO journal **32**(12): 1717-1729.

Danaei, G., M. M. Finucane, et al. (2011). "National, regional, and global trends in fasting plasma glucose and diabetes prevalence since 1980: systematic analysis of health

examination surveys and epidemiological studies with 370 country-years and 2.7 million participants." Lancet **378**(9785): 31-40.

Demetriades, C., N. Doumpas, et al. (2014). "Regulation of TORC1 in Response to Amino Acid Starvation via Lysosomal Recruitment of TSC2." Cell **156**(4): 786-799.

Dibble, C. C., W. Elis, et al. (2012). "TBC1D7 is a third subunit of the TSC1-TSC2 complex upstream of mTORC1." Molecular cell **47**(4): 535-546.

Duran, R. V., W. Oppliger, et al. (2012). "Glutaminolysis activates Rag-mTORC1 signaling." Molecular cell **47**(3): 349-358.

Duvel, K., J. L. Yecies, et al. (2010). "Activation of a metabolic gene regulatory network downstream of mTOR complex 1." Molecular cell **39**(2): 171-183.

Ebato, C., T. Uchida, et al. (2008). "Autophagy is important in islet homeostasis and compensatory increase of beta cell mass in response to high-fat diet." Cell metabolism **8**(4): 325-332.

Efeyan, A., R. Zoncu, et al. (2013). "Regulation of mTORC1 by the Rag GTPases is necessary for neonatal autophagy and survival." Nature **493**(7434): 679-683.

Eisler, S. A., Y. F. Fuchs, et al. (2012). "G-PKDrep-live, a genetically encoded FRET reporter to measure PKD activity at the trans-Golgi-network." Biotechnology journal **7**(1): 148-154.

English, L., M. Chemali, et al. (2009). "Autophagy enhances the presentation of endogenous viral antigens on MHC class I molecules during HSV-1 infection." Nature immunology **10**(5): 480-487.

Eskelinen, E. L., F. Reggiori, et al. (2011). "Seeing is believing: the impact of electron microscopy on autophagy research." Autophagy **7**(9): 935-956.

Findlay, G. M., L. Yan, et al. (2007). "A MAP4 kinase related to Ste20 is a nutrient-sensitive regulator of mTOR signalling." The Biochemical journal **403**(1): 13-20.

Fujimoto, K., P. T. Hanson, et al. (2009). "Autophagy regulates pancreatic beta cell death in response to Pdx1 deficiency and nutrient deprivation." The Journal of biological chemistry **284**(40): 27664-27673.

Fujita, N., T. Itoh, et al. (2008). "The Atg16L complex specifies the site of LC3 lipidation for membrane biogenesis in autophagy." Molecular biology of the cell **19**(5): 2092-2100.

Fujitani, Y., T. Ueno, et al. (2010). "Autophagy in health and disease. 4. The role of pancreatic beta-cell autophagy in health and diabetes." American journal of physiology. Cell physiology **299**(1): C1-6.

Ganley, I. G., H. Lam du, et al. (2009). "ULK1.ATG13.FIP200 complex mediates mTOR signaling and is essential for autophagy." The Journal of biological chemistry **284**(18): 12297-12305.

Garami, A., F. J. Zwartkruis, et al. (2003). "Insulin activation of Rheb, a mediator of mTOR/S6K/4E-BP signaling, is inhibited by TSC1 and 2." Molecular cell **11**(6): 1457-1466.

Gehart, H., A. Goginashvili, et al. (2012). "The BAR domain protein Arfaptin-1 controls secretory granule biogenesis at the trans-Golgi network." Developmental cell **23**(4): 756-768.

Gold, G., M. L. Gishizky, et al. (1982). "Evidence that glucose "marks" beta cells resulting in preferential release of newly synthesized insulin." Science **218**(4567): 56-58.

Gong, R., L. Li, et al. (2011). "Crystal structure of the Gtr1p-Gtr2p complex reveals new insights into the amino acid-induced TORC1 activation." Genes & development **25**(16): 1668-1673.

Goodge, K. A. and J. C. Hutton (2000). "Translational regulation of proinsulin biosynthesis and proinsulin conversion in the pancreatic beta-cell." Seminars in cell & developmental biology **11**(4): 235-242.

Gremlich, S., C. Nolan, et al. (2005). "Pancreatic islet adaptation to fasting is dependent on peroxisome proliferator-activated receptor alpha transcriptional up-regulation of fatty acid oxidation." Endocrinology **146**(1): 375-382.

Gwinn, D. M., D. B. Shackelford, et al. (2008). "AMPK phosphorylation of raptor mediates a metabolic checkpoint." Molecular cell **30**(2): 214-226.

Hailey, D. W., A. S. Rambold, et al. (2010). "Mitochondria supply membranes for autophagosome biogenesis during starvation." Cell **141**(4): 656-667.

Halban, P. A. (1982). "Differential rates of release of newly synthesized and of stored insulin from pancreatic islets." Endocrinology **110**(4): 1183-1188.

Hamasaki, M., N. Furuta, et al. (2013). "Autophagosomes form at ER-mitochondria contact sites." Nature **495**(7441): 389-393.

Han, D., S. Moon, et al. (2012). "Comprehensive phosphoproteome analysis of INS-1 pancreatic beta-cells using various digestion strategies coupled with liquid chromatography-tandem mass spectrometry." Journal of proteome research **11**(4): 2206-2223.

Han, J. M., S. J. Jeong, et al. (2012). "Leucyl-tRNA synthetase is an intracellular leucine sensor for the mTORC1-signaling pathway." Cell **149**(2): 410-424.

Hara, K., K. Yonezawa, et al. (1998). "Amino acid sufficiency and mTOR regulate p70 S6 kinase and eIF-4E BP1 through a common effector mechanism." The Journal of biological chemistry **273**(23): 14484-14494.

Hara, T., K. Nakamura, et al. (2006). "Suppression of basal autophagy in neural cells causes neurodegenerative disease in mice." Nature **441**(7095): 885-889.

Harding, T. M., A. Hefner-Gravink, et al. (1996). "Genetic and phenotypic overlap between autophagy and the cytoplasm to vacuole protein targeting pathway." The Journal of biological chemistry **271**(30): 17621-17624.

Hausser, A., G. Link, et al. (2002). "Structural requirements for localization and activation of protein kinase C mu (PKC mu) at the Golgi compartment." The Journal of cell biology **156**(1): 65-74.

Hayashi-Nishino, M., N. Fujita, et al. (2009). "A subdomain of the endoplasmic reticulum forms a cradle for autophagosome formation." Nature cell biology **11**(12): 1433-1437.

Hosokawa, N., T. Hara, et al. (2009). "Nutrient-dependent mTORC1 association with the ULK1-Atg13-FIP200 complex required for autophagy." Molecular biology of the cell **20**(7): 1981-1991.

Hou, N., H. Mogami, et al. (2012). "Preferential release of newly synthesized insulin assessed by a multi-label reporter system using pancreatic beta-cell line MIN6." PloS one **7**(10): e47921.

Howell, J. J., S. J. Ricoult, et al. (2013). "A growing role for mTOR in promoting anabolic metabolism." Biochemical Society transactions **41**(4): 906-912.

Hsu, P. P., S. A. Kang, et al. (2011). "The mTOR-regulated phosphoproteome reveals a mechanism of mTORC1-mediated inhibition of growth factor signaling." Science **332**(6035): 1317-1322.

Ichimura, Y., T. Kirisako, et al. (2000). "A ubiquitin-like system mediates protein lipidation." Nature **408**(6811): 488-492.

Inoki, K., Y. Li, et al. (2003). "Rheb GTPase is a direct target of TSC2 GAP activity and regulates mTOR signaling." Genes & development **17**(15): 1829-1834.

Itakura, E., C. Kishi-Itakura, et al. (2012). "The hairpin-type tail-anchored SNARE syntaxin 17 targets to autophagosomes for fusion with endosomes/lysosomes." Cell **151**(6): 1256-1269.

Jung, C. H., C. B. Jun, et al. (2009). "ULK-Atg13-FIP200 complexes mediate mTOR signaling to the autophagy machinery." Molecular biology of the cell **20**(7): 1992-2003.

Jung, H. S., K. W. Chung, et al. (2008). "Loss of autophagy diminishes pancreatic beta cell mass and function with resultant hyperglycemia." Cell metabolism **8**(4): 318-324.

Kabeya, Y., N. Mizushima, et al. (2000). "LC3, a mammalian homologue of yeast Apg8p, is localized in autophagosome membranes after processing." The EMBO journal **19**(21): 5720-5728.

Kabeya, Y., N. Mizushima, et al. (2004). "LC3, GABARAP and GATE16 localize to autophagosomal membrane depending on form-II formation." Journal of cell science **117**(Pt 13): 2805-2812.

Kang, S. A., M. E. Pacold, et al. (2013). "mTORC1 phosphorylation sites encode their sensitivity to starvation and rapamycin." Science **341**(6144): 1236566.

Kawasome, H., P. Papst, et al. (1998). "Targeted disruption of p70(s6k) defines its role in protein synthesis and rapamycin sensitivity." Proceedings of the National Academy of Sciences of the United States of America **95**(9): 5033-5038.

Kihara, A., Y. Kabeya, et al. (2001). "Beclin-phosphatidylinositol 3-kinase complex functions at the trans-Golgi network." EMBO reports **2**(4): 330-335.

Kim, E., P. Goraksha-Hicks, et al. (2008). "Regulation of TORC1 by Rag GTPases in nutrient response." Nature cell biology **10**(8): 935-945.

Kim, J., M. Kundu, et al. (2011). "AMPK and mTOR regulate autophagy through direct phosphorylation of Ulk1." Nature cell biology **13**(2): 132-141.

Kim, S. G., G. R. Buel, et al. (2013). "Nutrient regulation of the mTOR complex 1 signaling pathway." Molecules and cells **35**(6): 463-473.

Kim, S. G., G. R. Hoffman, et al. (2013). "Metabolic stress controls mTORC1 lysosomal localization and dimerization by regulating the TTT-RUVBL1/2 complex." Molecular cell **49**(1): 172-185.

Kimura, S., T. Noda, et al. (2007). "Dissection of the autophagosome maturation process by a novel reporter protein, tandem fluorescent-tagged LC3." Autophagy **3**(5): 452-460.

Kirisako, T., Y. Ichimura, et al. (2000). "The reversible modification regulates the membrane-binding state of Apg8/Aut7 essential for autophagy and the cytoplasm to vacuole targeting pathway." The Journal of cell biology **151**(2): 263-276.

Komatsu, M., S. Waguri, et al. (2005). "Impairment of starvation-induced and constitutive autophagy in Atg7-deficient mice." The Journal of cell biology **169**(3): 425-434.

Koren, I., E. Reem, et al. (2010). "DAP1, a novel substrate of mTOR, negatively regulates autophagy." Current biology : CB **20**(12): 1093-1098.

Kuma, A. and N. Mizushima (2010). "Physiological role of autophagy as an intracellular recycling system: with an emphasis on nutrient metabolism." Seminars in cell & developmental biology **21**(7): 683-690.

Lamb, C. A., T. Yoshimori, et al. (2013). "The autophagosome: origins unknown, biogenesis complex." Nature reviews. Molecular cell biology **14**(12): 759-774.

Laplante, M. and D. M. Sabatini (2012). "mTOR signaling in growth control and disease." Cell **149**(2): 274-293.

Lenormand, C., C. Spiegelhalter, et al. (2013). "Birbeck granule-like "organized smooth endoplasmic reticulum" resulting from the expression of a cytoplasmic YFP-tagged langerin." PloS one **8**(4): e60813.

Lewis, C. A., B. Griffiths, et al. (2011). "Regulation of the SREBP transcription factors by mTORC1." Biochemical Society transactions **39**(2): 495-499.

Li, X., L. Zhang, et al. (2006). "Islet microvasculature in islet hyperplasia and failure in a model of type 2 diabetes." Diabetes **55**(11): 2965-2973.

Liljedahl, M., Y. Maeda, et al. (2001). "Protein kinase D regulates the fission of cell surface destined transport carriers from the trans-Golgi network." Cell **104**(3): 409-420.

Masini, M., M. Bugliani, et al. (2009). "Autophagy in human type 2 diabetes pancreatic beta cells." Diabetologia **52**(6): 1083-1086.

McAlpine, F., L. E. Williamson, et al. (2013). "Regulation of nutrient-sensitive autophagy by uncoordinated 51-like kinases 1 and 2." Autophagy **9**(3): 361-373.

Menon, S., C. C. Dibble, et al. (2014). "Spatial Control of the TSC Complex Integrates Insulin and Nutrient Regulation of mTORC1 at the Lysosome." Cell **156**(4): 771-785.

Michael, D. J., W. Xiong, et al. (2007). "Human insulin vesicle dynamics during pulsatile secretion." Diabetes **56**(5): 1277-1288.

Mizushima, N. and M. Komatsu (2011). "Autophagy: renovation of cells and tissues." Cell **147**(4): 728-741.

Mizushima, N., A. Kuma, et al. (2003). "Mouse Apg16L, a novel WD-repeat protein, targets to the autophagic isolation membrane with the Apg12-Apg5 conjugate." Journal of cell science **116**(Pt 9): 1679-1688.

Mizushima, N., H. Sugita, et al. (1998). "A new protein conjugation system in human. The counterpart of the yeast Apg12p conjugation system essential for autophagy." The Journal of biological chemistry **273**(51): 33889-33892.

Mizushima, N., A. Yamamoto, et al. (2001). "Dissection of autophagosome formation using Apg5-deficient mouse embryonic stem cells." The Journal of cell biology **152**(4): 657-668.

Mizushima, N., A. Yamamoto, et al. (2004). "In vivo analysis of autophagy in response to nutrient starvation using transgenic mice expressing a fluorescent autophagosome marker." Molecular biology of the cell **15**(3): 1101-1111.

Mizushima, N., T. Yoshimori, et al. (2011). "The role of Atg proteins in autophagosome formation." Annual review of cell and developmental biology **27**: 107-132.

Nakai, A., O. Yamaguchi, et al. (2007). "The role of autophagy in cardiomyocytes in the basal state and in response to hemodynamic stress." Nature medicine **13**(5): 619-624.

Nazio, F., F. Strappazzon, et al. (2013). "mTOR inhibits autophagy by controlling ULK1 ubiquitylation, self-association and function through AMBRA1 and TRAF6." Nature cell biology **15**(4): 406-416.

Nicklin, P., P. Bergman, et al. (2009). "Bidirectional transport of amino acids regulates mTOR and autophagy." Cell **136**(3): 521-534.

Nishida, Y., S. Arakawa, et al. (2009). "Discovery of Atg5/Atg7-independent alternative macroautophagy." Nature **461**(7264): 654-658.

Nobukuni, T., M. Joaquin, et al. (2005). "Amino acids mediate mTOR/raptor signaling through activation of class 3 phosphatidylinositol 3OH-kinase." Proceedings of the National Academy of Sciences of the United States of America **102**(40): 14238-14243.

Novikoff, A. B. (1959). "The proximal tubule cell in experimental hydronephrosis." The Journal of biophysical and biochemical cytology **6**(1): 136-138.

Novikoff, A. B., H. Beaufay, et al. (1956). "Electron microscopy of lysosomerich fractions from rat liver." The Journal of biophysical and biochemical cytology **2**(4 Suppl): 179-184.

Ogmundsdottir, M. H., S. Heublein, et al. (2012). "Proton-assisted amino acid transporter PAT1 complexes with Rag GTPases and activates TORC1 on late endosomal and lysosomal membranes." PloS one **7**(5): e36616.

Oshiro, N., J. Rapley, et al. (2014). "Amino Acids Activate Mammalian Target of Rapamycin (mTOR) Complex 1 without Changing Rag GTPase Guanyl Nucleotide Charging." The Journal of biological chemistry **289**(5): 2658-2674.

Owen, J. L., Y. Zhang, et al. (2012). "Insulin stimulation of SREBP-1c processing in transgenic rat hepatocytes requires p70 S6-kinase." Proceedings of the National Academy of Sciences of the United States of America **109**(40): 16184-16189.

Panchaud, N., M. P. Peli-Gulli, et al. (2013). "Amino acid deprivation inhibits TORC1 through a GTPase-activating protein complex for the Rag family GTPase Gtr1." Science signaling **6**(277): ra42.

Panchaud, N., M. P. Peli-Gulli, et al. (2013). "SEACing the GAP that nEGOCiates TORC1 activation: evolutionary conservation of Rag GTPase regulation." Cell cycle **12**(18): 2948-2952.

Pearson, R. B., P. B. Dennis, et al. (1995). "The principal target of rapamycin-induced p70s6k inactivation is a novel phosphorylation site within a conserved hydrophobic domain." The EMBO journal **14**(21): 5279-5287.

Peterson, T. R., S. S. Sengupta, et al. (2011). "mTOR complex 1 regulates lipin 1 localization to control the SREBP pathway." Cell **146**(3): 408-420.

Polson, H. E., J. de Lartigue, et al. (2010). "Mammalian Atg18 (WIPI2) localizes to omegasome-anchored phagophores and positively regulates LC3 lipidation." Autophagy **6**(4): 506-522.

Porstmann, T., C. R. Santos, et al. (2008). "SREBP activity is regulated by mTORC1 and contributes to Akt-dependent cell growth." Cell metabolism **8**(3): 224-236.

Pouli, A. E., E. Emmanouilidou, et al. (1998). "Secretory-granule dynamics visualized in vivo with a phogrin-green fluorescent protein chimaera." The Biochemical journal **333 (Pt 1)**: 193-199.

Prentki, M., F. M. Matschinsky, et al. (2013). "Metabolic signaling in fuel-induced insulin secretion." Cell metabolism **18**(2): 162-185.

Quan, W., K. Y. Hur, et al. (2012). "Autophagy deficiency in beta cells leads to compromised unfolded protein response and progression from obesity to diabetes in mice." Diabetologia **55**(2): 392-403.

Rabinowitz, J. D. and E. White (2010). "Autophagy and metabolism." Science **330**(6009): 1344-1348.

Ravier, M. A., M. Nenquin, et al. (2009). "Glucose controls cytosolic Ca2+ and insulin secretion in mouse islets lacking adenosine triphosphate-sensitive K+ channels owing to a knockout of the pore-forming subunit Kir6.2." Endocrinology **150**(1): 33-45.

Ravikumar, B., K. Moreau, et al. (2010). "Plasma membrane contributes to the formation of pre-autophagosomal structures." Nature cell biology **12**(8): 747-757.

Robitaille, A. M., S. Christen, et al. (2013). "Quantitative phosphoproteomics reveal mTORC1 activates de novo pyrimidine synthesis." Science **339**(6125): 1320-1323.

Rorsman, P. and M. Braun (2013). "Regulation of insulin secretion in human pancreatic islets." Annual review of physiology **75**: 155-179.

Russell, R. C., Y. Tian, et al. (2013). "ULK1 induces autophagy by phosphorylating Beclin-1 and activating VPS34 lipid kinase." Nature cell biology **15**(7): 741-750.

Sancak, Y., L. Bar-Peled, et al. (2010). "Ragulator-Rag complex targets mTORC1 to the lysosomal surface and is necessary for its activation by amino acids." Cell **141**(2): 290-303.

Sancak, Y., T. R. Peterson, et al. (2008). "The Rag GTPases bind raptor and mediate amino acid signaling to mTORC1." Science **320**(5882): 1496-1501.

Sandberg, M. and L. A. Borg (2006). "Intracellular degradation of insulin and crinophagy are maintained by nitric oxide and cyclo-oxygenase 2 activity in isolated pancreatic islets." Biology of the cell / under the auspices of the European Cell Biology Organization **98**(5): 307-315.

Saucedo, L. J., X. Gao, et al. (2003). "Rheb promotes cell growth as a component of the insulin/TOR signalling network." Nature cell biology **5**(6): 566-571.

Scarlatti, F., R. Maffei, et al. (2008). "Role of non-canonical Beclin 1-independent autophagy in cell death induced by resveratrol in human breast cancer cells." Cell death and differentiation **15**(8): 1318-1329.

Schlumpberger, M., E. Schaeffeler, et al. (1997). "AUT1, a gene essential for autophagocytosis in the yeast Saccharomyces cerevisiae." Journal of bacteriology **179**(4): 1068-1076.

Shang, L., S. Chen, et al. (2011). "Nutrient starvation elicits an acute autophagic response mediated by Ulk1 dephosphorylation and its subsequent dissociation from AMPK." Proceedings of the National Academy of Sciences of the United States of America **108**(12): 4788-4793.

Sharlow, E. R., K. V. Giridhar, et al. (2008). "Potent and selective disruption of protein kinase D functionality by a benzoxoloazepinolone." The Journal of biological chemistry **283**(48): 33516-33526.

Shintani, T. and D. J. Klionsky (2004). "Autophagy in health and disease: a double-edged sword." Science **306**(5698): 990-995.

Shoji-Kawata, S., R. Sumpter, et al. (2013). "Identification of a candidate therapeutic autophagy-inducing peptide." Nature **494**(7436): 201-206.

Shpilka, T., H. Weidberg, et al. (2011). "Atg8: an autophagy-related ubiquitin-like protein family." Genome biology **12**(7): 226.

Smith, R. E. and M. G. Farquhar (1966). "Lysosome function in the regulation of the secretory process in cells of the anterior pituitary gland." The Journal of cell biology **31**(2): 319-347.

Steiner, D. F. (2011). "On the discovery of precursor processing." Methods in molecular biology **768**: 3-11.

Steiner, D. F., D. Cunningham, et al. (1967). "Insulin biosynthesis: evidence for a precursor." Science **157**(3789): 697-700.

Stocker, H., T. Radimerski, et al. (2003). "Rheb is an essential regulator of S6K in controlling cell growth in Drosophila." Nature cell biology **5**(6): 559-565.

Sumara, G., I. Formentini, et al. (2009). "Regulation of PKD by the MAPK p38delta in insulin secretion and glucose homeostasis." Cell **136**(2): 235-248.

Szollosi, A., M. Nenquin, et al. (2007). "Glucose stimulates Ca2+ influx and insulin secretion in 2-week-old beta-cells lacking ATP-sensitive K+ channels." The Journal of biological chemistry **282**(3): 1747-1756.

Szollosi, A., M. Nenquin, et al. (2007). "Overnight culture unmasks glucose-induced insulin secretion in mouse islets lacking ATP-sensitive K+ channels by improving the triggering Ca2+ signal." The Journal of biological chemistry **282**(20): 14768-14776.

Takeshige, K., M. Baba, et al. (1992). "Autophagy in yeast demonstrated with proteinase-deficient mutants and conditions for its induction." The Journal of cell biology **119**(2): 301-311.

Tanida, I., T. Ueno, et al. (2004). "LC3 conjugation system in mammalian autophagy." The international journal of biochemistry & cell biology **36**(12): 2503-2518.

Thoreen, C. C., L. Chantranupong, et al. (2012). "A unifying model for mTORC1-mediated regulation of mRNA translation." Nature **485**(7396): 109-113.

Thumm, M., R. Egner, et al. (1994). "Isolation of autophagocytosis mutants of Saccharomyces cerevisiae." FEBS letters **349**(2): 275-280.

Tsukada, M. and Y. Ohsumi (1993). "Isolation and characterization of autophagy-defective mutants of Saccharomyces cerevisiae." FEBS letters **333**(1-2): 169-174.

Tsun, Z. Y., L. Bar-Peled, et al. (2013). "The folliculin tumor suppressor is a GAP for the RagC/D GTPases that signal amino acid levels to mTORC1." Molecular cell **52**(4): 495-505.

Wang, X., W. Li, et al. (2001). "Regulation of elongation factor 2 kinase by p90(RSK1) and p70 S6 kinase." The EMBO journal **20**(16): 4370-4379.

Weidberg, H., E. Shvets, et al. (2010). "LC3 and GATE-16/GABARAP subfamilies are both essential yet act differently in autophagosome biogenesis." The EMBO journal **29**(11): 1792-1802.

Whiting, D. R., L. Guariguata, et al. (2011). "IDF diabetes atlas: global estimates of the prevalence of diabetes for 2011 and 2030." Diabetes research and clinical practice **94**(3): 311-321.

Wicksteed, B., T. P. Herbert, et al. (2001). "Cooperativity between the preproinsulin mRNA untranslated regions is necessary for glucose-stimulated translation." The Journal of biological chemistry **276**(25): 22553-22558.

Williams, A., S. Sarkar, et al. (2008). "Novel targets for Huntington's disease in an mTOR-independent autophagy pathway." Nature chemical biology **4**(5): 295-305.

Wong, P. M., C. Puente, et al. (2013). "The ULK1 complex: sensing nutrient signals for autophagy activation." Autophagy **9**(2): 124-137.

Wullschleger, S., R. Loewith, et al. (2006). "TOR signaling in growth and metabolism." Cell **124**(3): 471-484.

Xu, L., D. Salloum, et al. (2011). "Phospholipase D mediates nutrient input to mammalian target of rapamycin complex 1 (mTORC1)." The Journal of biological chemistry **286**(29): 25477-25486.

Yamamoto, A., R. Masaki, et al. (1990). "Characterization of the isolation membranes and the limiting membranes of autophagosomes in rat hepatocytes by lectin cytochemistry." The journal of histochemistry and cytochemistry : official journal of the Histochemistry Society **38**(4): 573-580.

Yamamoto, A., Y. Tagawa, et al. (1998). "Bafilomycin A1 prevents maturation of autophagic vacuoles by inhibiting fusion between autophagosomes and lysosomes in rat hepatoma cell line, H-4-II-E cells." Cell structure and function **23**(1): 33-42.

Yla-Anttila, P., H. Vihinen, et al. (2009). "3D tomography reveals connections between the phagophore and endoplasmic reticulum." Autophagy **5**(8): 1180-1185.

Yla-Anttila, P., H. Vihinen, et al. (2009). "Monitoring autophagy by electron microscopy in Mammalian cells." Methods in enzymology **452**: 143-164.

Yoon, M. S., G. Du, et al. (2011). "Class III PI-3-kinase activates phospholipase D in an amino acid-sensing mTORC1 pathway." The Journal of cell biology **195**(3): 435-447.

Young, A. R., E. Y. Chan, et al. (2006). "Starvation and ULK1-dependent cycling of mammalian Atg9 between the TGN and endosomes." Journal of cell science **119**(Pt 18): 3888-3900.

Yu, L., C. K. McPhee, et al. (2010). "Termination of autophagy and reformation of lysosomes regulated by mTOR." Nature **465**(7300): 942-946.

Yuan, H. X., Y. Xiong, et al. (2013). "Nutrient sensing, metabolism, and cell growth control." Molecular cell **49**(3): 379-387.

Zhong, Y., Q. J. Wang, et al. (2009). "Distinct regulation of autophagic activity by Atg14L and Rubicon associated with Beclin 1-phosphatidylinositol-3-kinase complex." Nature cell biology **11**(4): 468-476.

Zoncu, R., L. Bar-Peled, et al. (2011). "mTORC1 senses lysosomal amino acids through an inside-out mechanism that requires the vacuolar H(+)-ATPase." Science **334**(6056): 678-683.